AERODYNAMIC CHARACTERISTICS OF A THREE-ENGINE SUPERSONIC TRANSPORT MODEL HAVING A LOW-ASPECT-RATIO VARIABLE-SWEEP WARPED WING

By Odell A. Morris and Dennis E. Fuller

Langley Research Center
Langley Station, Hampton, Va.

NATIONAL AERONAUTICS AND SPACE ADMINISTRATION

AERODYNAMIC CHARACTERISTICS OF A THREE-ENGINE SUPERSONIC TRANSPORT MODEL HAVING A LOW-ASPECT-RATIO VARIABLE-SWEEP WARPED WING*

By Odell A. Morris and Dennis E. Fuller
Langley Research Center

SUMMARY

16595

An investigation has been conducted in the Langley Unitary Plan wind tunnel at Mach numbers of 2.40, 2.60, and 2.96 to determine the longitudinal and lateral aerodynamic characteristics of a model of a variable-sweep supersonic transport configuration with a design Mach number of 2.6 (SCAT 16-B). The three-engine configuration had a low-aspect-ratio wing with a leading-edge sweep angle of 76°. Two of the engine nacelles were mounted below the wing and one was mounted in the vertical tail. The investigation also included tests on the configuration with three different wing glove shapes.

The results indicated that for the basic model configuration, the maximum trimmed lift-drag ratios varied from about 6.0 at a Mach number of 2.40 to about 5.8 and 5.7 at Mach numbers of 2.60 and 2.96, respectively. The twist and camber distribution of the wing-body combination was such that the configuration was completely self-trimmed at the lift coefficient for maximum lift-drag ratios for Mach numbers of 2.40 and 2.60. Reducing the sweep angle of the wing glove resulted in an increase in the static margin with the greatest increase occurring for the 70° wing glove. A body modification which increased the body width in the region of the wing leading edge provided a considerable increase in body volume with no decrease in performance.

The configuration indicated adequate longitudinal and directional stability and a positive effective dihedral for the angle-of-attack range required for cruising flight. In comparison with the original SCAT 16 model, the present basic configuration had slightly higher values of maximum lift-drag ratio and considerably higher static margin.

INTRODUCTION

The National Aeronautics and Space Administration has an intensive research program underway to provide the research background necessary to define and meet the design requirements for a commercially acceptable supersonic transport airplane. Results of some of the initial studies have been reported in

*Title, Unclassified.

references 1 to 6. The investigation of references 5 and 6 reports the results on a three-engine variable-sweep supersonic transport configuration designed for a Mach number of 2.6 (SCAT 16). This configuration employed a high-aspect-ratio wing and was found to have undesirable pitch-up characteristics in the low speed range. Also the performance level in the supersonic speed range was such that further improvement would be required.

Thus, in an effort to improve the configuration, several modifications to the model were made and tested. The modifications consisted primarily of the following: The high aspect ratio of the wing was reduced with a view toward improving the structural characteristics of the wing; the inboard wing leading edge was adapted for tests with three different wing glove shapes aimed at improving the low-speed pitch-up characteristics by varying the sweep angles; and the two side-mounted fuselage nacelles were relocated and mounted in a position below the wing to improve the lift and drag interference effects. In addition, the negative dihedral of the horizontal tail was reduced from -20° to 0°.

Tests of the modified configuration (SCAT 16-B) were conducted at Mach numbers of 2.40, 2.60, and 2.96 over an angle-of-attack range from about -4° to 10° and an angle-of-sideslip range from about -4° to 6° for several angles of attack. The Reynolds number of the tests was 3.0×10^6 per foot for each Mach number. Results of the investigation, together with a limited analysis, are presented herein.

SYMBOLS

All results are referred to the body-axis system except those for the lift and drag coefficients, which are referred to the stability-axis system. The moment reference point is at a longitudinal station corresponding to 62.3 percent of the body length. The coefficients are based on the geometry of the 16° swept wing (ref. 5).

b	reference wing span, in.
C_D	drag coefficient, Drag/qS
C_L	lift coefficient, Lift/qS
C_l	rolling-moment coefficient, Rolling moment/qSb
C_{l_β}	effective-dihedral parameter, $\partial C_l/\partial\beta$
C_m	pitching-moment coefficient, Pitching moment/qSc
$\frac{\partial C_m}{\partial C_L}$	longitudinal-stability parameter (measured at zero lift coefficient)

C_n	yawing-moment coefficient, Yawing moment/qSb
C_{n_β}	directional-stability parameter, $\partial C_n/\partial\beta$
C_Y	side-force coefficient, Side force/qS
C_{Y_β}	side-force parameter, $\partial C_Y/\partial\beta$
c	reference wing chord, in.
L/D	lift-drag ratio
M	free-stream Mach number
q	free-stream dynamic pressure, lb/sq ft
S	reference wing area of 16° swept wing, sq ft
t	local thickness
α	angle of attack, deg
β	angle of sideslip, deg
δ_h	horizontal-tail deflection, positive when trailing edge is down, deg
Λ	sweep angle of wing glove leading edge, deg

Subscripts:

max	maximum
min	minimum
trim	trimmed condition

Model component designations:

B	original body shape
B_M	modified body shape
E_1	engine nacelle mounted in vertical tail
E_3	two engine nacelles mounted under wing and one engine nacelle mounted in vertical tail
Glove 1	76° swept wing glove

Glove 2 70° swept wing glove

Glove 3 65° swept wing glove

MODEL AND APPARATUS

Details and dimensions of the model and the various components are shown in figure 1 and table I. This configuration, which is designated as SCAT 16-B, is actually a modified version of the original SCAT 16 model, which is described in detail in reference 6. In comparison with the original SCAT 16 model, the present model has a different wing planform which has a considerably reduced span and an increased chord which was designed primarily to improve the structural characteristics of the wing. In the region of the wing-body juncture, the fixed section of the wing trailing edge was swept forward 25° and was extended below the variable-sweep wing panel to provide a suitable mounting location for the two engine nacelles below the wing.

The model was constructed so that three different wing glove shapes could be installed on the model as shown in figure 1. In changing the sweep angle of the wing glove shape from 76° to 65°, it should be noted that the location of the juncture of the fuselage and the wing leading edge was shifted rearward with corresponding small changes in wing area.

During the investigation a body fairing was added to the fuselage as shown in figure 1 to improve the normal area distribution of the model with the 70° wing glove.

The model was mounted in the tunnel on a remote-controlled sting, and force measurements were made through the use of a six-component internally mounted strain-gage balance.

TESTS, CORRECTIONS, AND ACCURACY

For all tests, the Reynolds number was 3.0×10^{6} per foot and the stagnation temperature was 150° F. The stagnation dewpoint was maintained sufficiently low to prevent condensation effects in the test section. Other test conditions are as follows:

Mach number	Stagnation pressure, lb/sq ft
2.40	2,405
2.60	2,679
2.96	3,247

Tests were made through an angle-of-attack range from about -4° to 10° and through a sideslip range from about -4° to 6°. The angles of attack and sideslip were corrected for the deflection of the balance and sting under load. Angles of attack were corrected for tunnel-flow misalinement. The balance-chamber and base pressures were measured, and the drag force was adjusted to a base pressure equal to free-stream static pressure. In addition, the drag results have been corrected for the internal skin-friction drag of the nacelles.

In order to assure a turbulent boundary layer, transition strips of No. 60 carborundum grit were applied 1/2 inch from the nose of the body and 1/2 inch (measured normal to the leading edge) from the leading edges of the wing and tails. Transition strips of No. 80 grit were applied on both the outer and inner surfaces of the engine nacelles 1/2 inch from the nose.

The estimated accuracy of the individual measured quantities is as follows:

C_L	±0.0020
C_D	±0.0004
C_m	±0.0004
C_l	±0.0002
C_n	±0.0002
C_Y	±0.0010
α, deg	±0.10
β, deg	±0.10

PRESENTATION OF RESULTS

The results of the investigation are presented in the following figures:

DISCUSSION

Longitudinal Aerodynamic Characteristics

The aerodynamic characteristics in pitch for the configuration with the original body shape and the three different wing glove shapes are shown in figure 2. In general, each of the configurations had adequate longitudinal stability for each test Mach number. The twist and camber distribution of the wing was such that the complete configuration displayed unusually good self-trimming characteristics. In fact, with wing glove shape 1 the model was completely self-trimmed at the lift coefficient for maximum lift-drag ratio at $M = 2.40$ and $M = 2.60$. At $M = 2.96$ the trim point was at a lift coefficient slightly beyond the maximum lift-drag ratio. The results indicated that for the basic model configuration, the maximum trimmed lift-drag ratios varied from about 6.0 at a Mach number of 2.40 to about 5.8 and 5.7 at Mach numbers of 2.60 and 2.96, respectively.

The largest effect of wing glove shape occurred for the pitching-moment data (fig. 2) wherein reducing the wing glove sweep from 76° to 70° considerably increased the longitudinal stability, probably because of the decrease in wing area forward of the pitch center. However, for the 65° wing glove, which had a slightly larger wing area than the 70° glove, the improvement in the longitudinal stability was less than that for the 70° glove, and at the highest lift coefficient tested showed a slight tendency toward pitch-up at $M = 2.40$. Effects of wing glove shape on the lift, drag, and lift-drag ratios were generally small; that is, the decrease in wing leading-edge sweep angle for wing gloves 2 and 3 produced small increases in drag with resulting small decreases in the lift-drag ratios of about 3 to 5 percent as might be expected.

The effects of horizontal-tail deflection are shown in figure 3 for the configuration with glove shape 1 and in figure 5 for the configuration with glove shape 2 and the modified body. The data indicate that deflection of the horizontal tail provides substantial control effectiveness for the configurations throughout the lift range.

The data of figure 4 shows the effect of the modified body shape on the aerodynamic characteristics in pitch for the configuration with wing glove 2.

Addition of the body fairing had only a small or negligible effect on the results although the fairing did provide a considerable increase in body volume. At a Mach number of 2.96 the small change in L/D due to the fairing was slightly beneficial.

The effects of the wing-mounted engine nacelles are shown in figure 6 for the configuration with the modified body shape and wing glove 2. Addition of the two engine nacelles under the wing produced a favorable lift increment at each Mach number which increased slightly with increasing angle of attack. The favorable lift increment tended to offset an unfavorable drag increment also produced by the nacelles; thus, only a small decrease in maximum lift-drag ratio resulted for the complete configuration.

A comparison of the longitudinal parameters for the original SCAT 16 (ref. 6) and the modified configurations of the present tests (SCAT 16-B) is presented in figure 7. It should be noted that the results presented in this figure are based on the reference area for the fully swept wing (76°) as was used for the SCAT 16 data of reference 6. The results show that the SCAT 16-B configuration with wing glove 1 has slightly higher maximum values of trimmed L/D than the SCAT 16 configuration and a considerably higher static margin. The static margin for the SCAT 16-B configuration with wing glove 2 was the highest of the three models and, as a result, the level of trimmed L/D was the lowest. However, to trim this configuration at a static margin of about 18 percent (which is comparable with the SCAT 16 level) would require a rearward shift in the pitching-moment reference of about 0.23c. The pitching-moment data of figure 5 indicate that a positive horizontal-tail deflection of about 2° would be required which would tend to improve the maximum trimmed L/D values for this configuration.

Lateral Aerodynamic Characteristics

The basic sideslip data presented in figure 8 for the configuration with the modified body shape and wing glove 2 indicate generally linear variations throughout the test sideslip-angle range for angles of attack of 0°, 5°, and 8°. The variations of the sideslip derivatives with angle of attack for the original configuration with the different wing glove shapes are presented in figure 9. The effect of changes in wing glove shape on the sideslip derivatives were small for each Mach number. The complete model with the different glove shapes maintains a reasonably good level of directional stability to angles of attack well above the region of maximum lift-drag ratio. However, increasing the angle of attack and Mach number tended to decrease C_{n_β} so that at $M = 2.96$, C_{n_β} decreased to zero at the highest angle of attack (10°). The variation of C_{l_β} with angle of attack was reasonably linear and indicates a positive effective dihedral for each configuration which tended to improve with increasing angle of attack.

The body modification (fig. 10) and horizontal-tail deflection (fig. 11) produced only small changes in the sideslip derivatives for the configuration with wing glove 2.

The addition of the two wing-mounted engine nacelles (fig. 12) produced a small stabilizing increment of C_{n_β} and increased the negative values of C_{l_β} and C_{Y_β}.

SUMMARY OF RESULTS

An investigation has been conducted in the Langley Unitary Plan wind tunnel at Mach numbers of 2.40, 2.60, and 2.96 to determine the longitudinal and lateral aerodynamic characteristics of a model of a variable-sweep supersonic transport configuration with a design Mach number of 2.6 (SCAT 16-B). The configuration had a highly swept wing with two engine nacelles mounted below the wing and one mounted in the vertical tail. The following results were indicated:

1. For the basic model configuration, the maximum trimmed lift-drag ratios varied from about 6.0 at a Mach number of 2.40 to about 5.8 and 5.7 at Mach numbers of 2.60 and 2.96, respectively. The twist and camber distribution of the wing-body combination was such that the configuration was completely self-trimmed at the lift coefficient for maximum lift-drag ratio at Mach numbers of 2.40 and 2.60.

2. Reducing the sweep angle of the wing glove resulted in an increase in the static margin with the greatest increase occurring for the 70° wing glove.

3. A body modification which increased the body width in the region of the wing leading edge provided a considerable increase in body volume with no decrease in performance.

4. In comparison with the original SCAT 16 model, the present basic configuration had a considerably higher static margin and a slightly higher maximum value of trimmed lift-drag ratio.

5. The configuration indicated adequate longitudinal and directional stability and a positive effective dihedral for the angle-of-attack range required for cruising flight.

Langley Research Center,
National Aeronautics and Space Administration,
Langley Station, Hampton, Va., June 12, 1964.

REFERENCES

1. Driver, Cornelius; Spearman, M. Leroy; and Corlett, William A.: Aerodynamic Characteristics at Mach Numbers From 1.61 to 2.86 of a Supersonic Transport Model With a Blended Wing-Body, Variable-Sweep Auxiliary Wing Panels, Outboard Tail Surfaces, and a Design Mach Number of 2.2. NASA TM X-817, 1963.

2. Robins, A. Warner; Spearman, M. Leroy; and Harris, Roy V., Jr.: Aerodynamic Characteristics at Mach Numbers of 2.30, 2.60, and 2.96 of a Supersonic Transport Model With a Blended Wing-Body, Variable-Sweep Auxiliary Wing Panels, Outboard Tail Surfaces, and a Design Mach Number of 2.6. NASA TM X-815, 1963.

3. Carraway, Ausley B.; Morris, Owen G.; and Carmel, Melvin M.: Aerodynamic Characteristics at Mach Numbers From 0.20 to 4.63 of a Canard-Type Supersonic Commercial Air Transport Configuration. NASA TM X-628, 1962.

4. Whitcomb, Richard T.; Patterson, James C., Jr.; and Kelly, Thomas C.: An Investigation of the Subsonic, Transonic, and Supersonic Aerodynamic Characteristics of a Proposed Arrow-Wing Transport Airplane Configuration. NASA TM X-800, 1963.

5. Lockwood, Vernard E.; McKinney, Linwood W.; and Lamar, John E.: Low-Speed Aerodynamic Characteristics of a Supersonic Transport Model With a High-Aspect-Ratio Variable-Sweep Warped Wing. NASA TM X-979, 1964.

6. Fuller, Dennis E.; and Weirich, Robert L.: Aerodynamic Characteristics at Mach Numbers From 0.50 to 2.96 of a Supersonic Transport Model With a Variable-Sweep High-Panel-Aspect-Ratio Wing. NASA TM X-980, 1964.

TABLE I.- GEOMETRIC CHARACTERISTICS OF 1/48-SCALE MODEL

Wing:	
Sweep of leading edge, deg	76.00
Wing t/c (mean), $\Lambda = 76^{\circ}$	0.045
Dihedral, $\Lambda = 76^{\circ}$	0.0
Aspect ratio, $\Lambda = 76^{\circ}$	1.255
Reference span, in., $\Lambda = 16^{\circ}$	33.45
Reference area, sq ft, $\Lambda = 16^{\circ}$	0.997
Reference wing chord, in., $\Lambda = 16^{\circ}$	5.77
Wing area, sq ft, $\Lambda = 76^{\circ}$	1.432
Fuselage:	
Length, in.	45.50
Base area, sq ft	0.02643
Horizontal tail:	
Exposed area, sq ft	0.2340
Span, in.	9.90
Circular-arc airfoil section, t/c	0.03
Dihedral	0.0
Vertical tail:	
Exposed area, sq ft	0.1515
Circular-arc airfoil section, t/c	0.03
Wing nacelles:	
Length, in.	7.50
Base area, sq ft (one)	0.00493
Capture area, sq ft (one)	0.00853
Vertical tail nacelle:	
Length, in.	7.92
Base area, sq ft	0.002816
Capture area, sq ft	0.01048

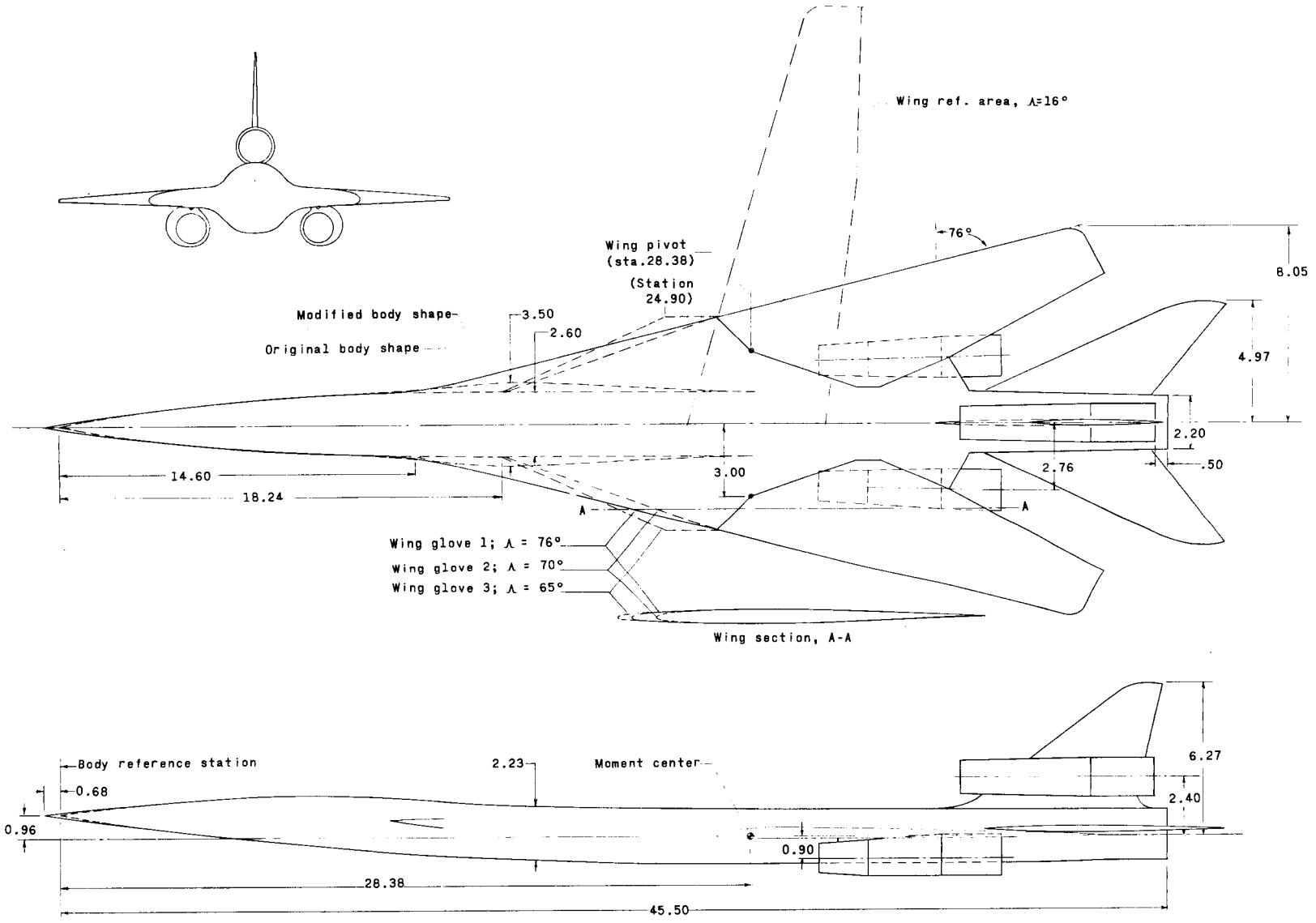

(a) Three-view drawing.

Figure 1.- Details of model. (All dimensions are in inches unless otherwise stated.)

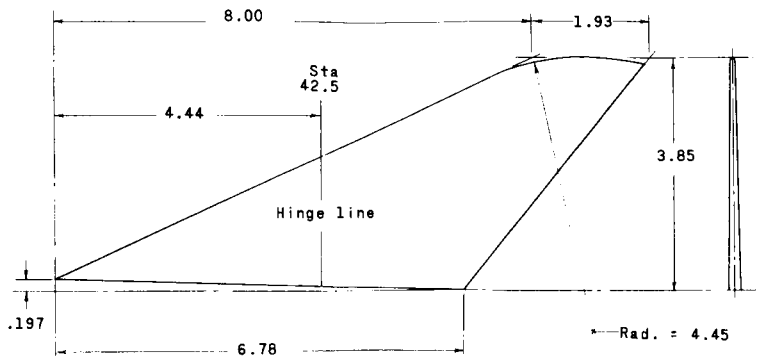

(b) Details of horizontal tail.

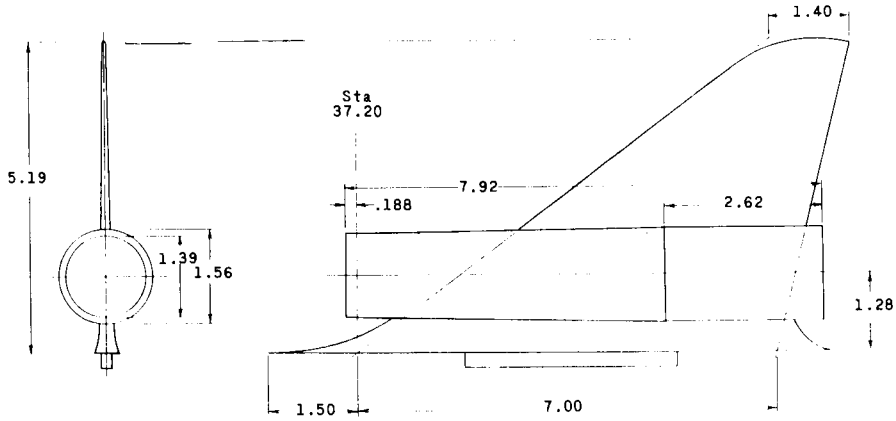

(c) Details of vertical tail with engine nacelle.

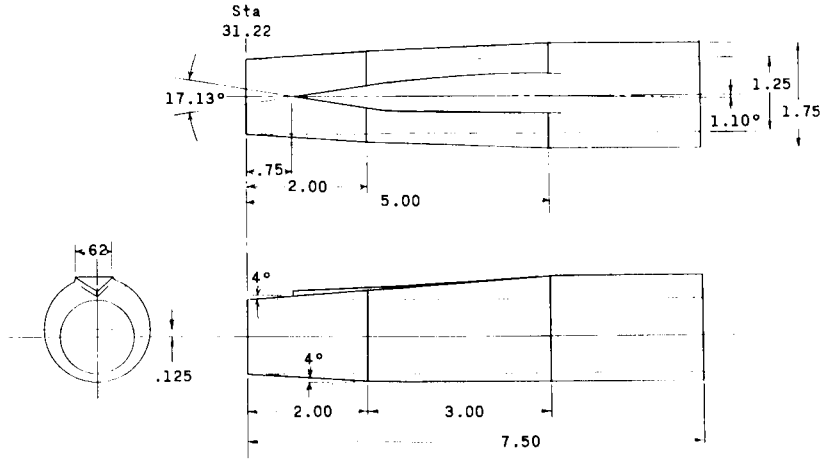

(d) Details of wing-mounted engine nacelles.

Figure 1.- Continued.

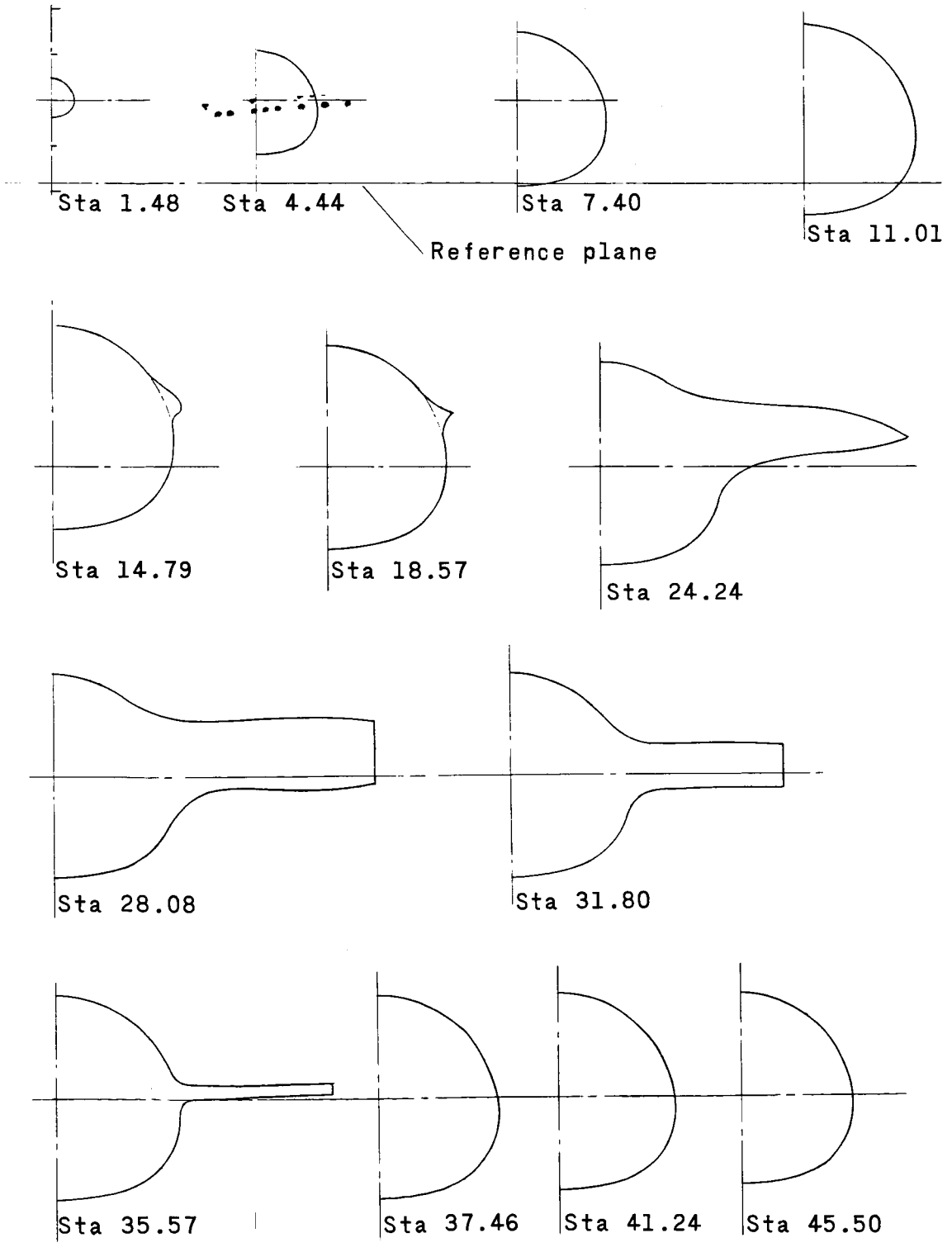

(e) Cross sections of various longitudinal stations.

Figure 1.- Concluded.

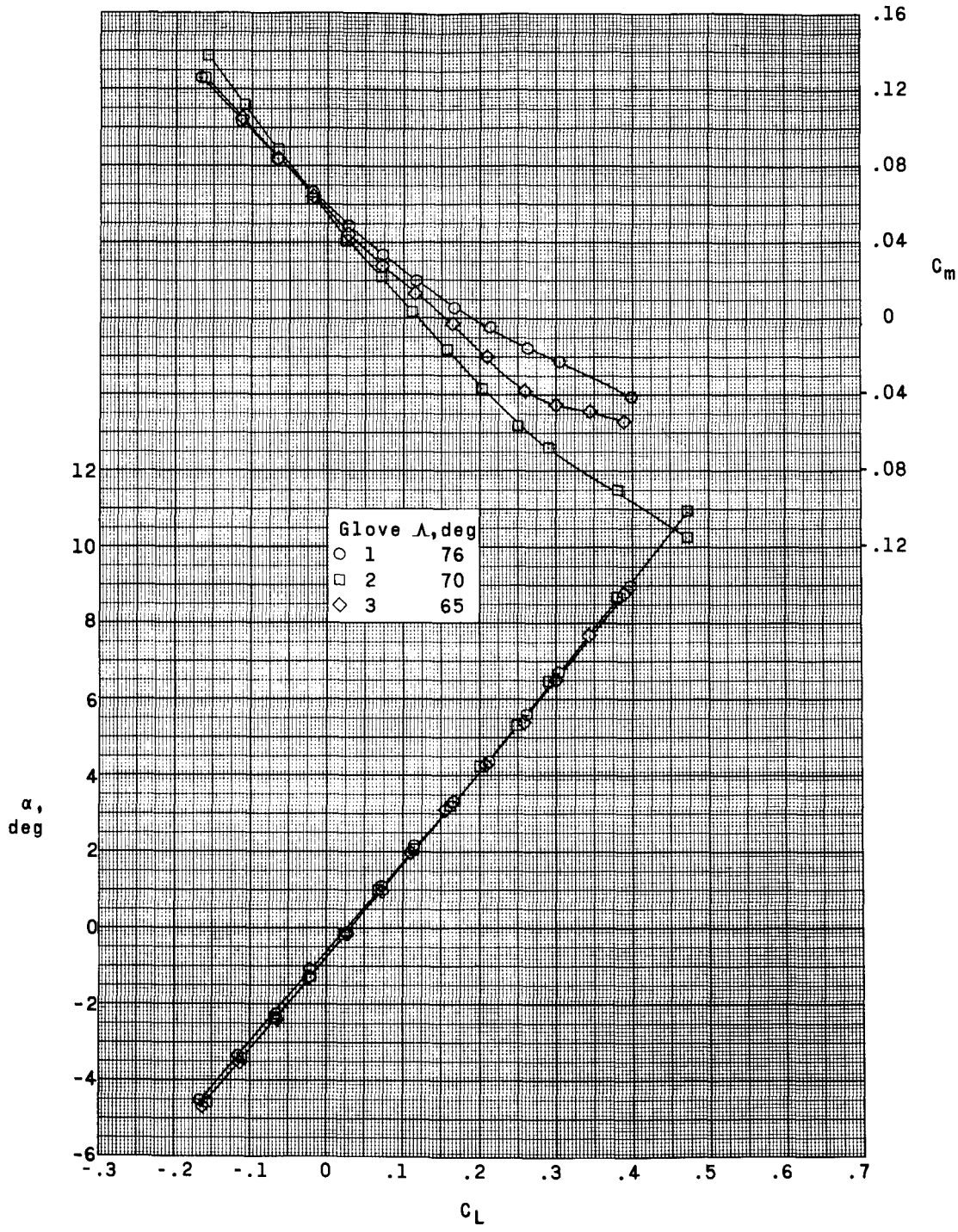

(a) M = 2.40.

Figure 2.- Effect of wing glove on the aerodynamic characteristics in pitch for the configuration with the original body shape.

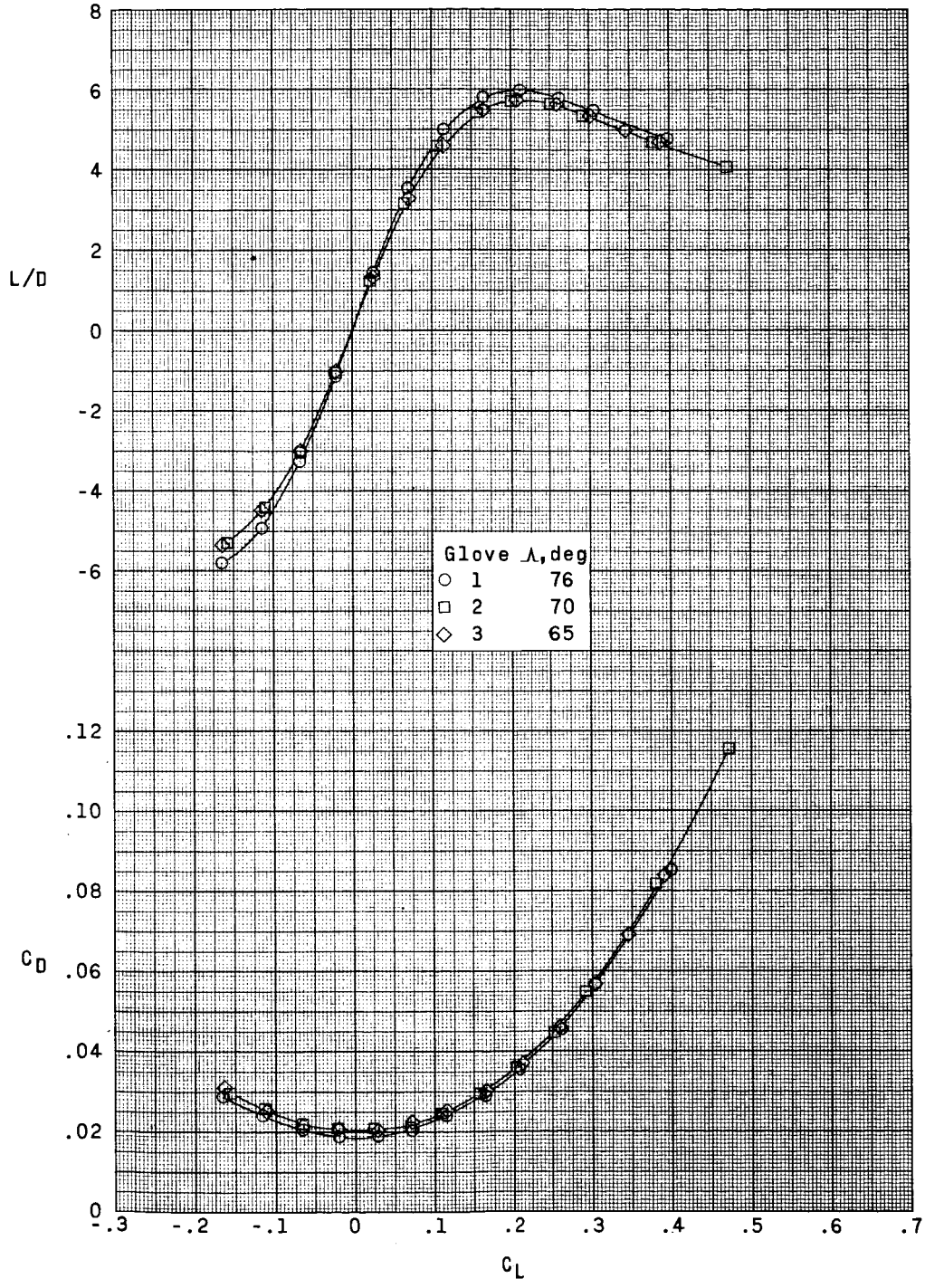

(a) Concluded.

Figure 2.- Continued.

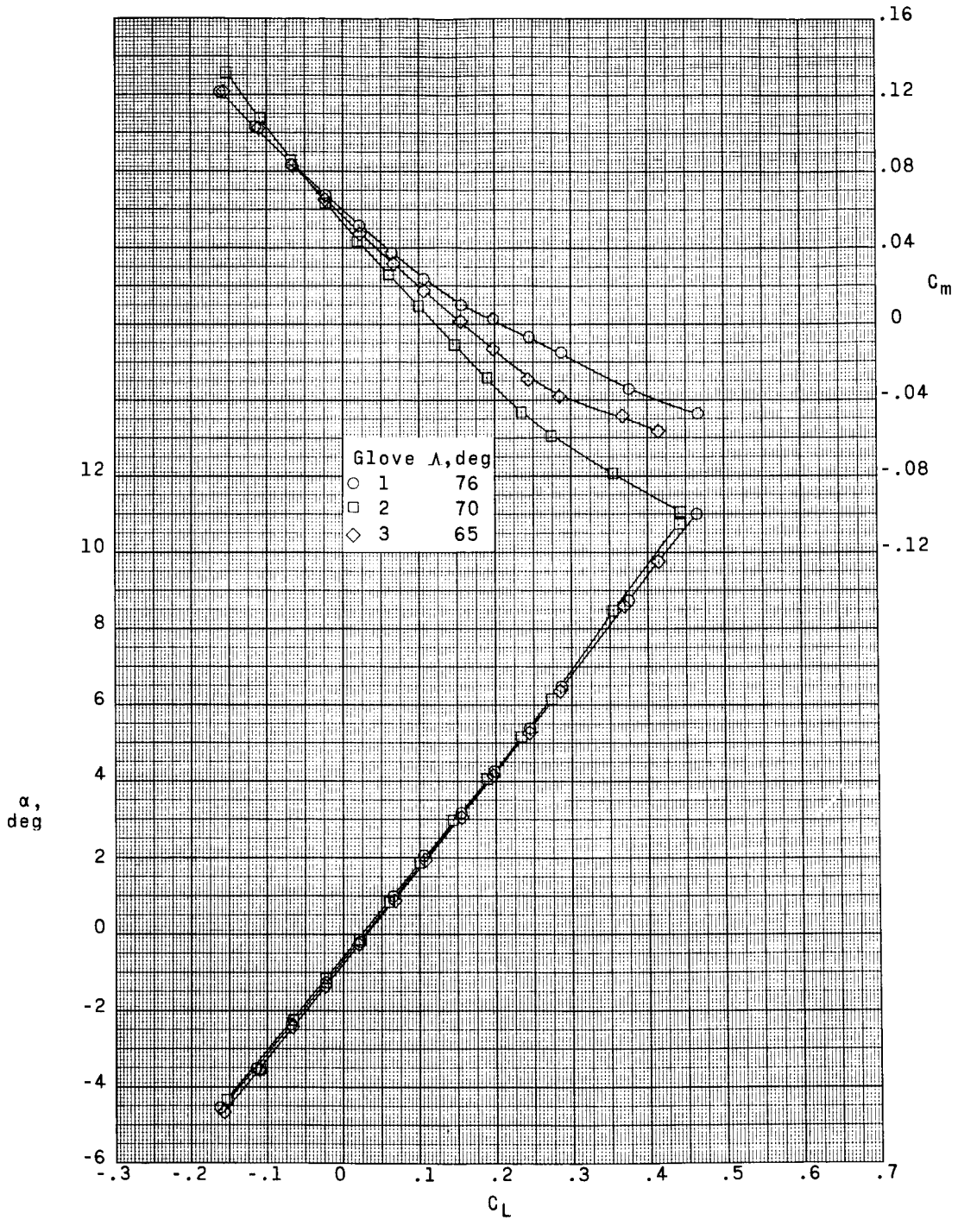

(b) M = 2.60.

Figure 2.- Continued.

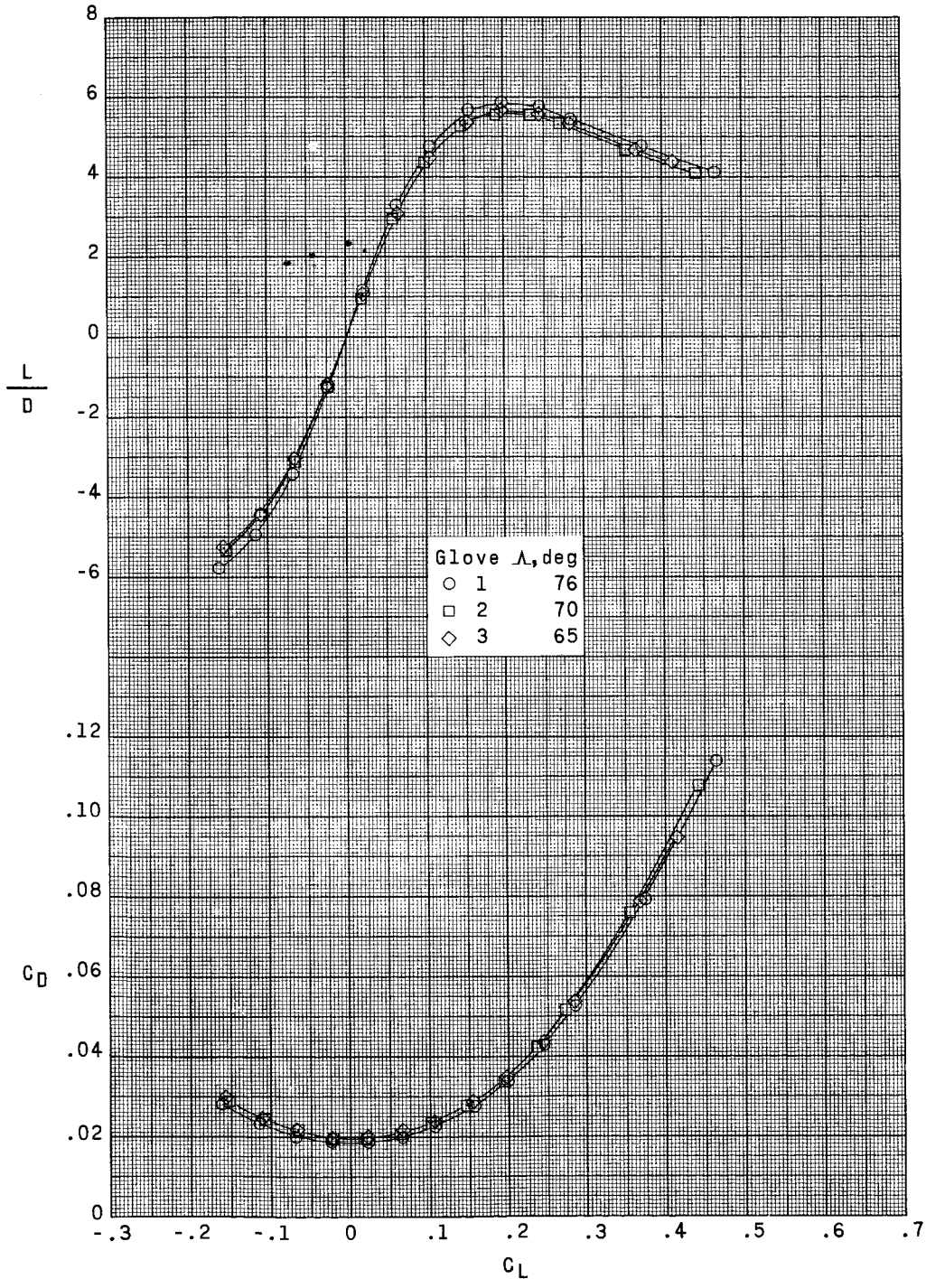

(b) Concluded.

Figure 2.- Continued.

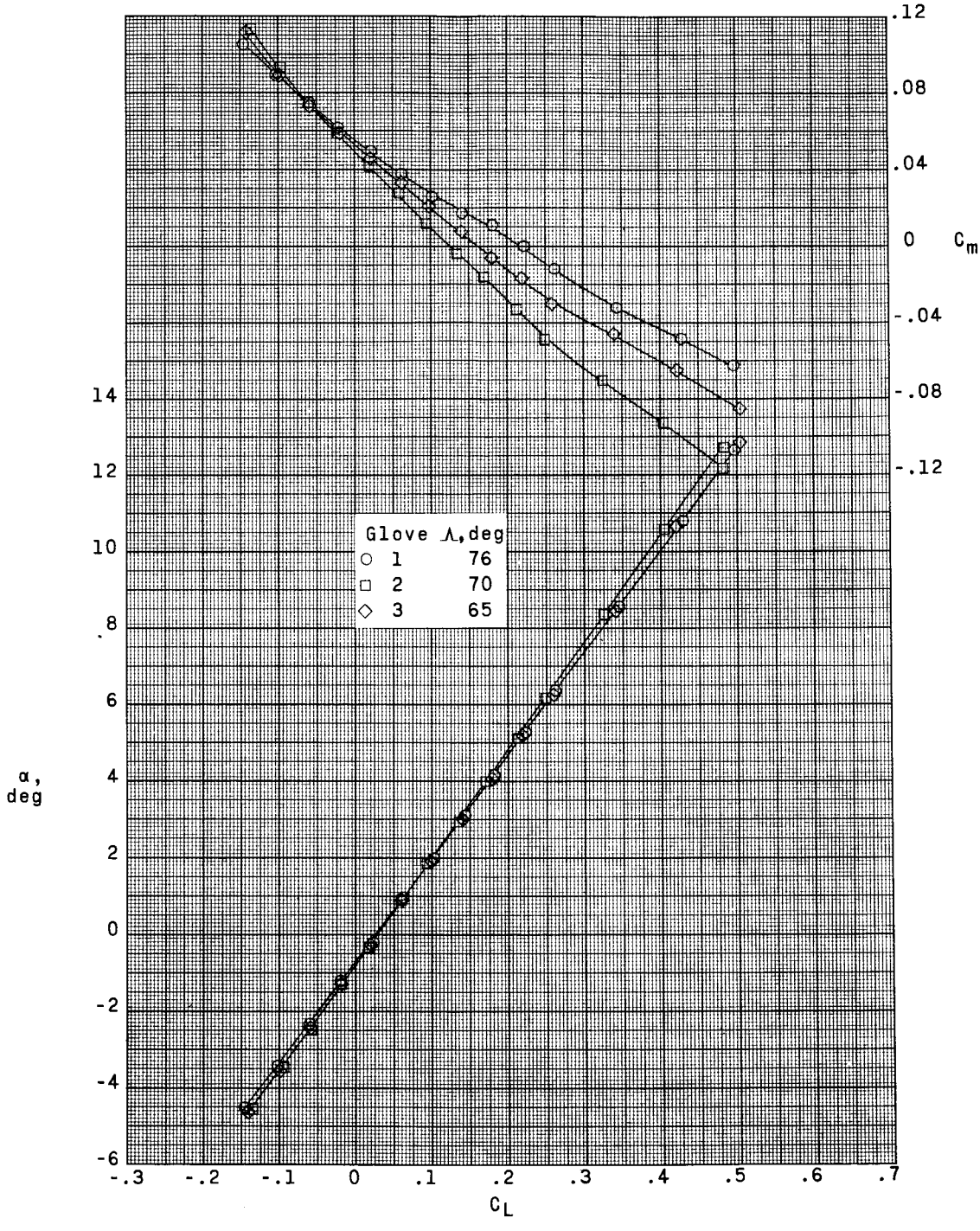

(c) M = 2.96.

Figure 2.- Continued.

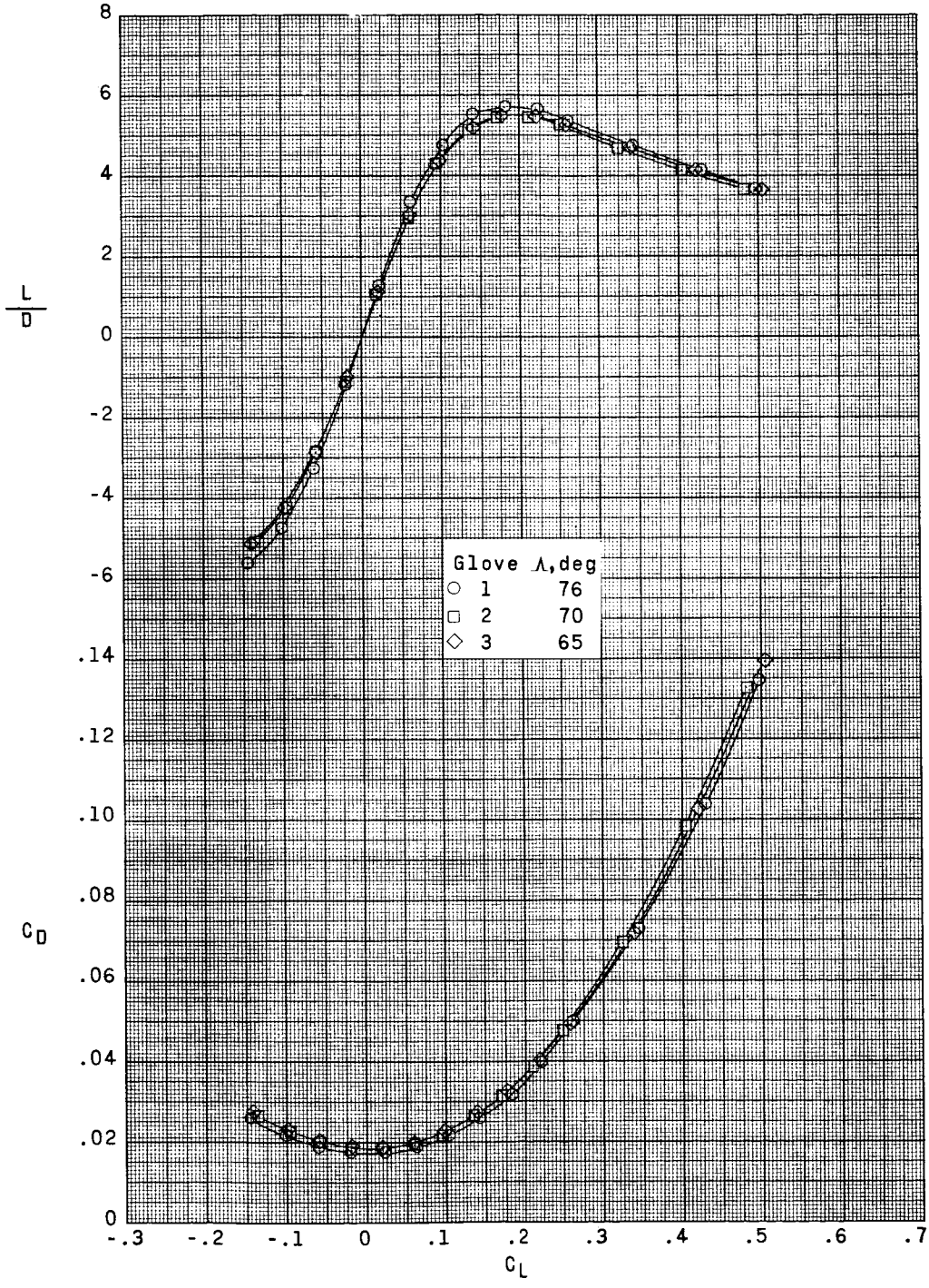

(c) Concluded.

Figure 2.- Concluded.

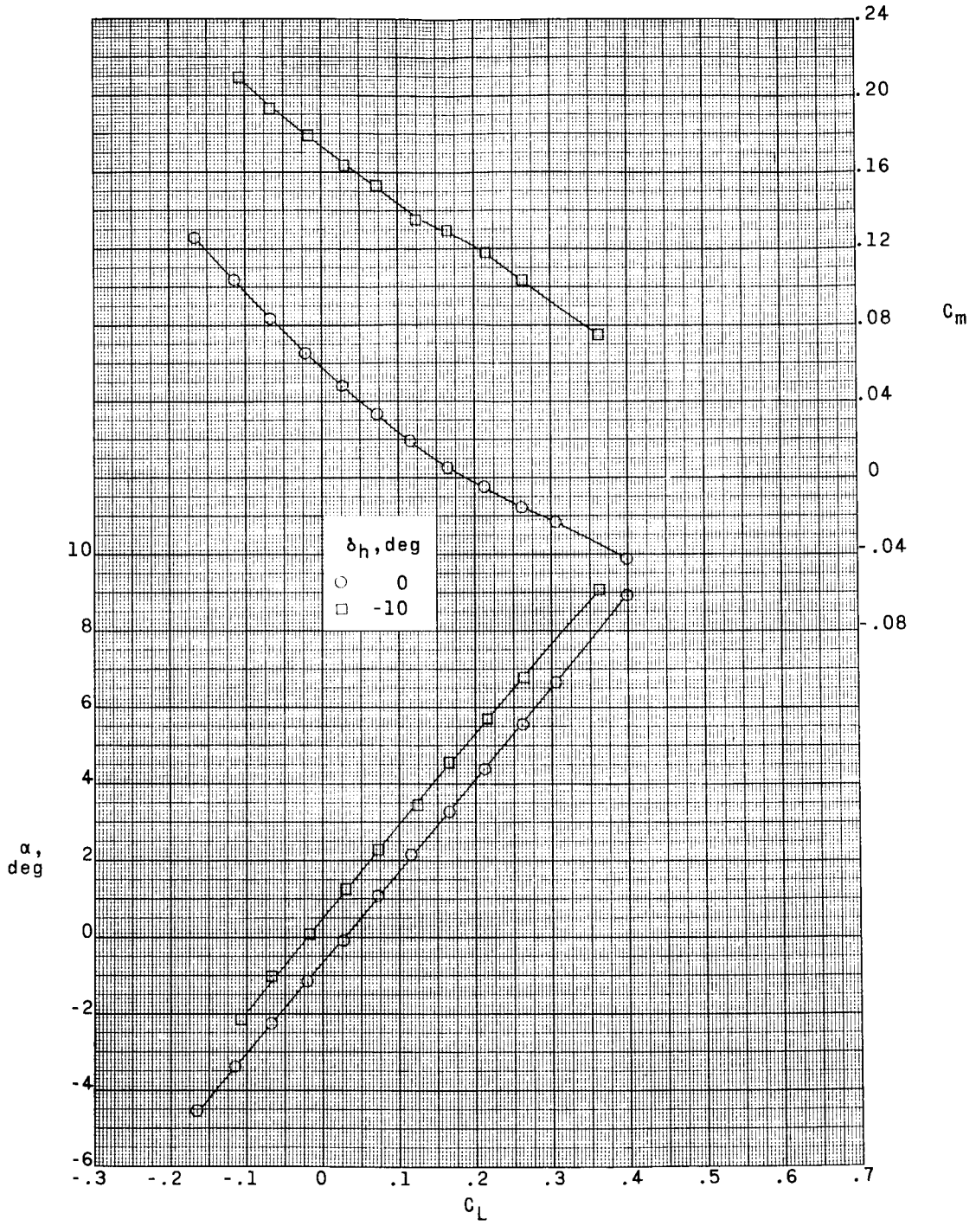

(a) M = 2.40.

Figure 3.- Effect of horizontal-tail deflection on the aerodynamic characteristics in pitch for the configuration with the original body shape and wing glove 1. $\Lambda = 76^{o}$.

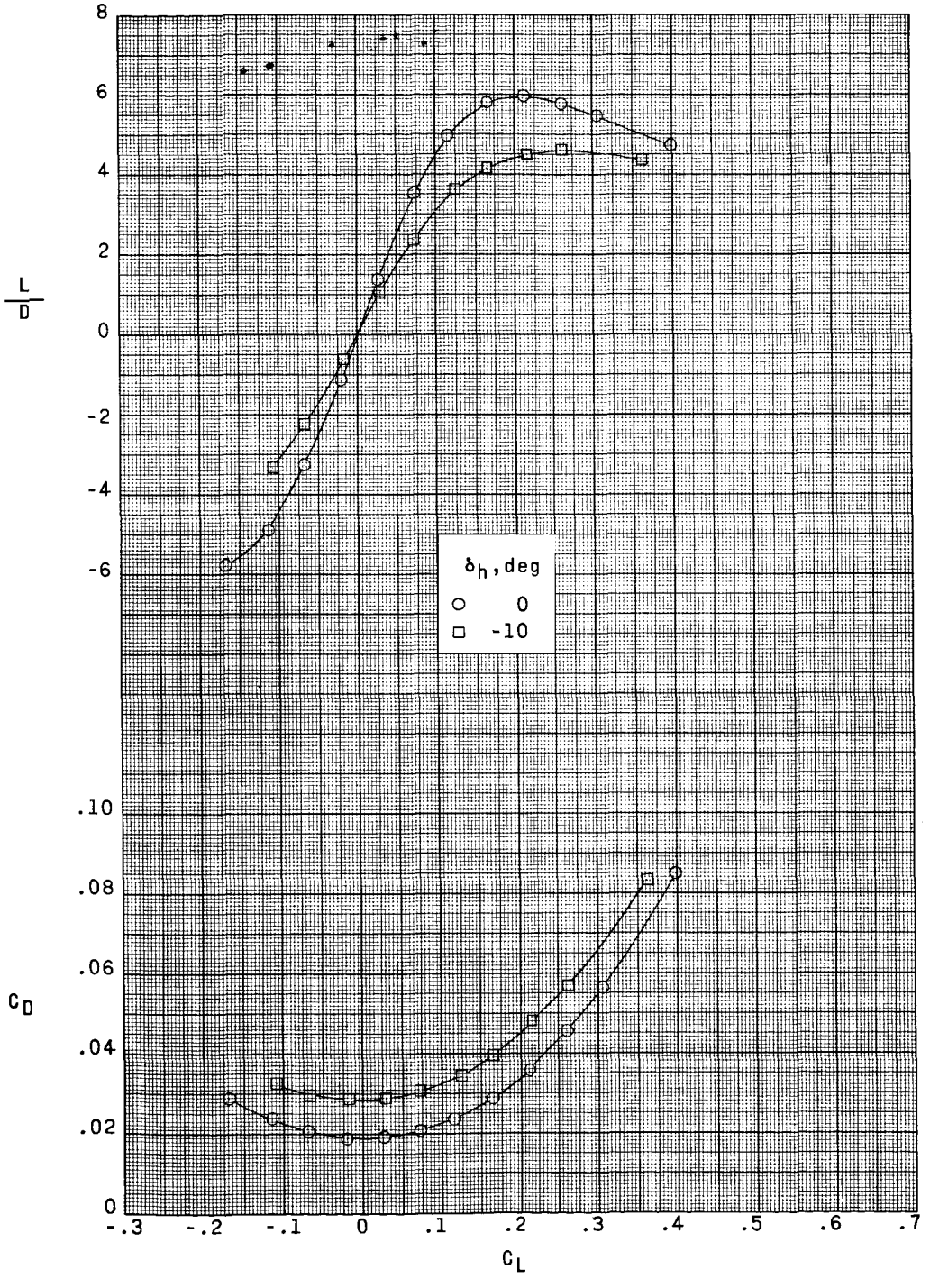

(a) Concluded.

Figure 3.- Continued.

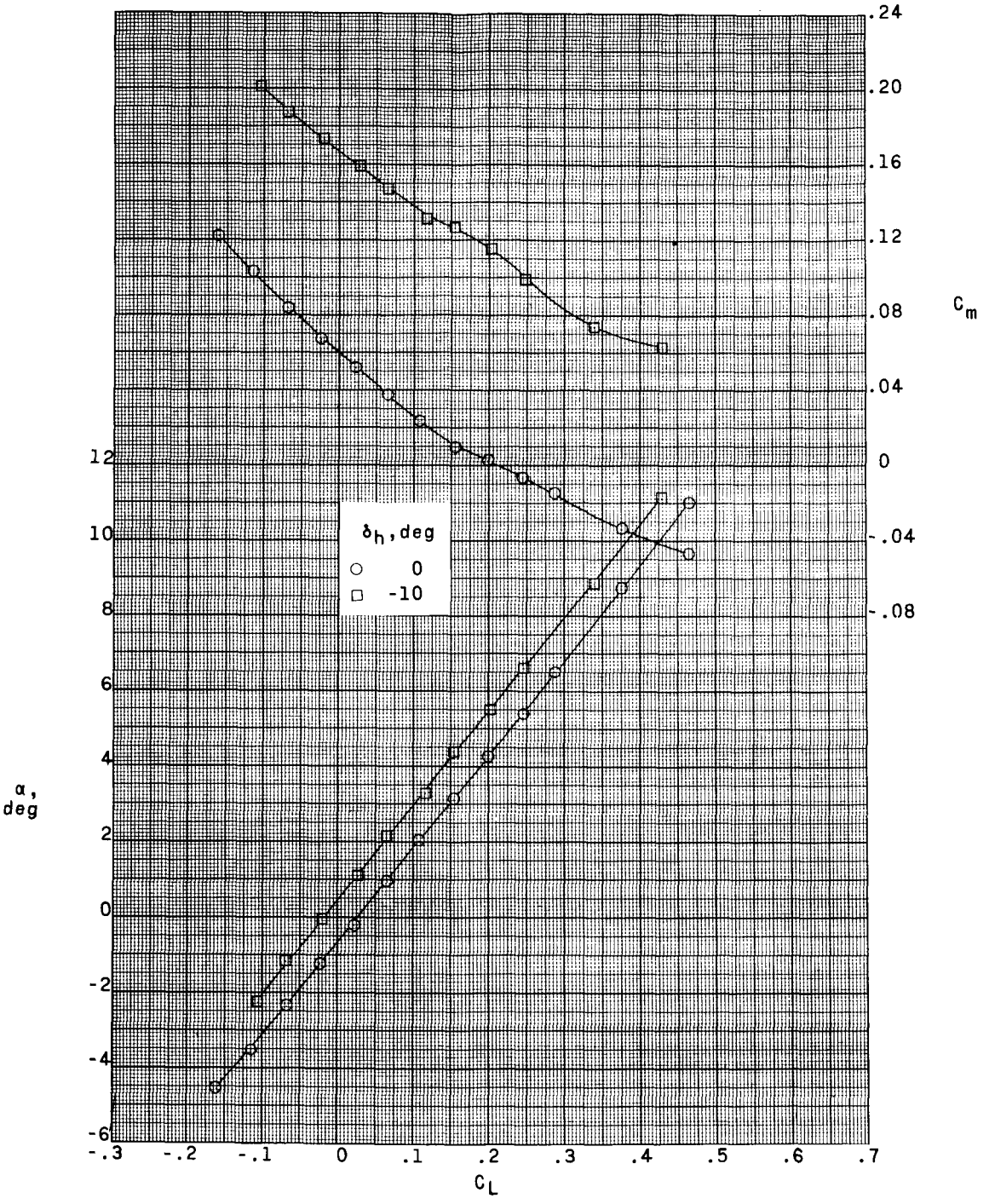

(b) M = 2.60.

Figure 3.- Continued.

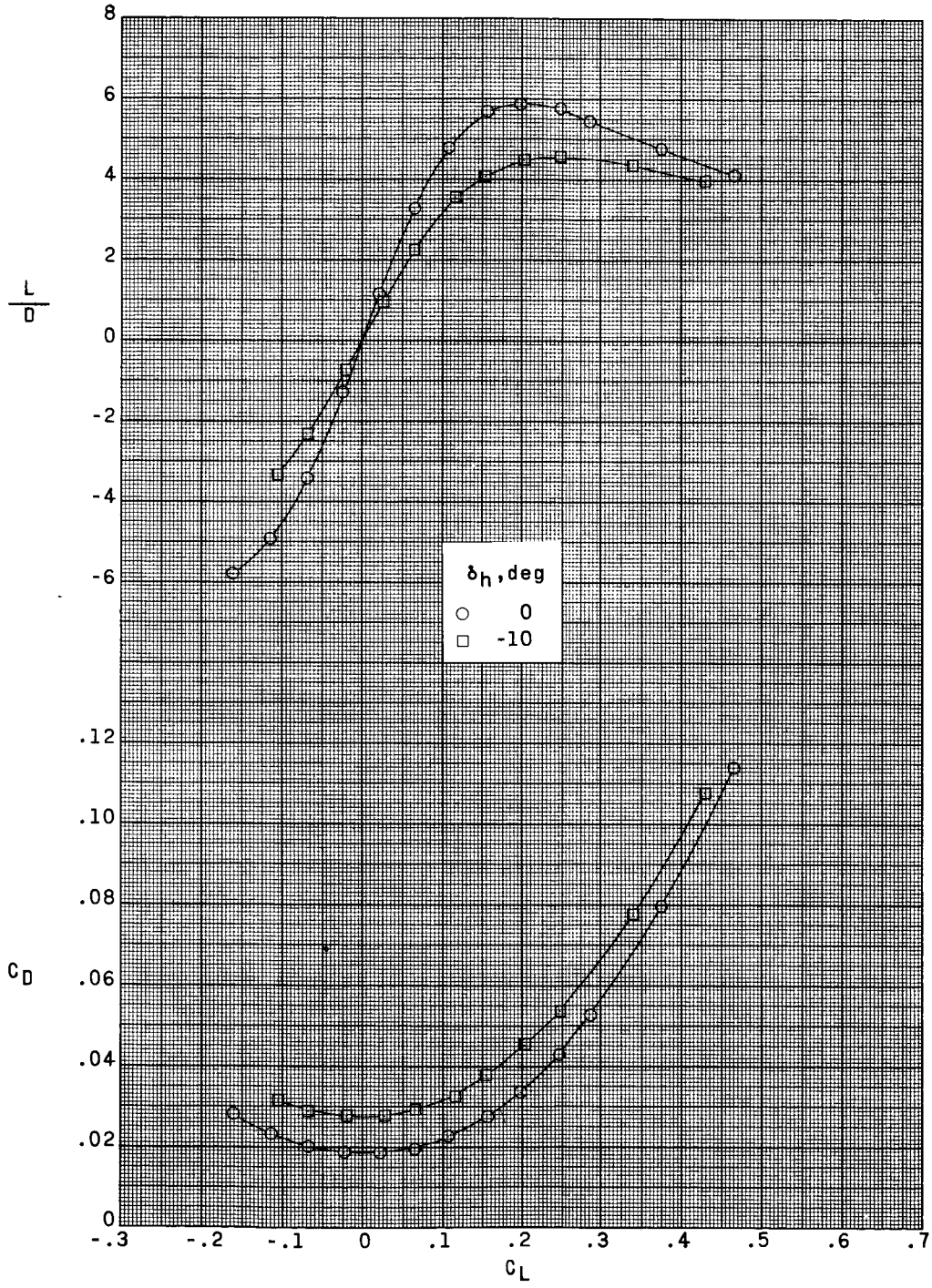

(b) Concluded.

Figure 3.- Continued.

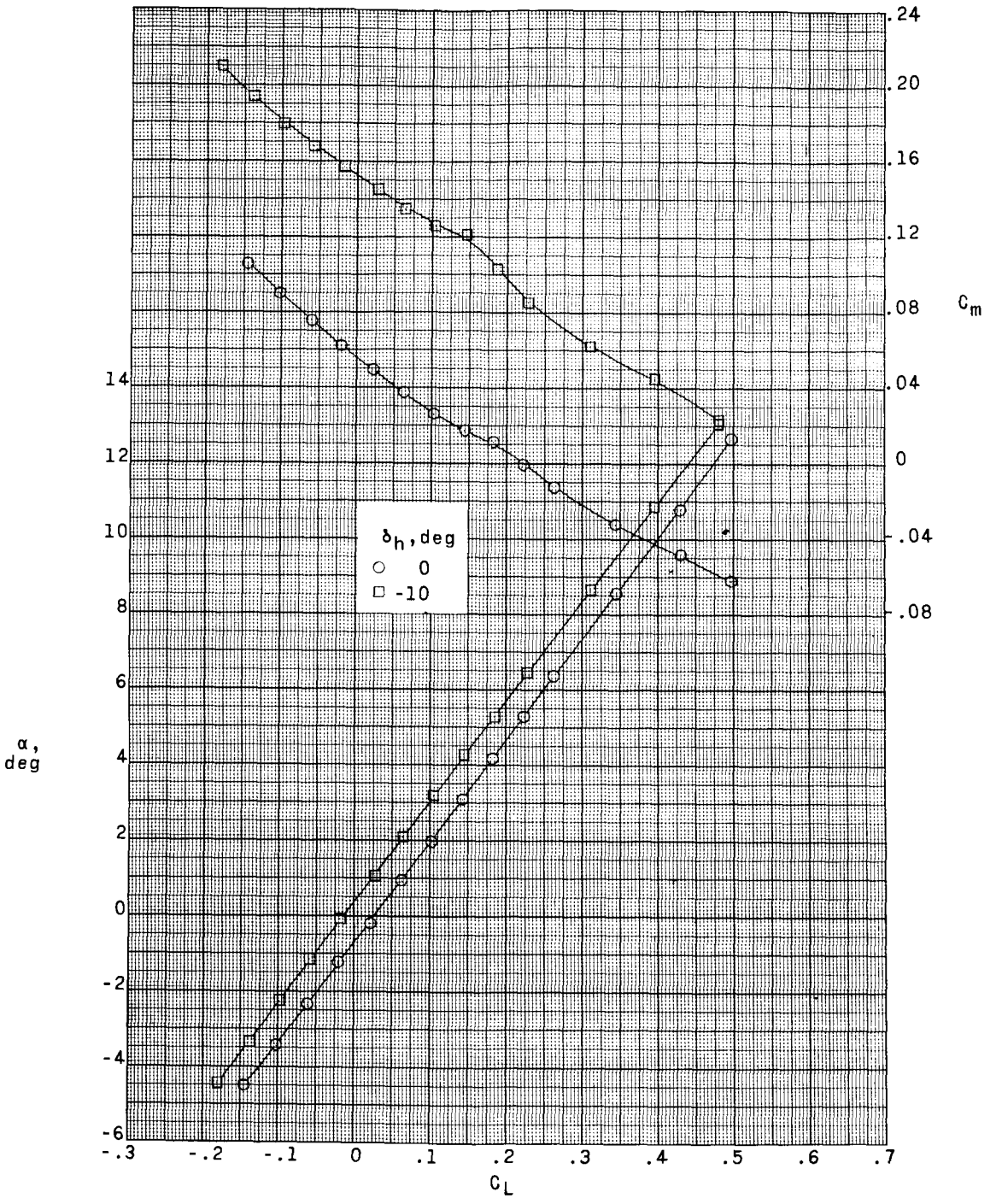

(c) M = 2.96.

Figure 3.- Continued.

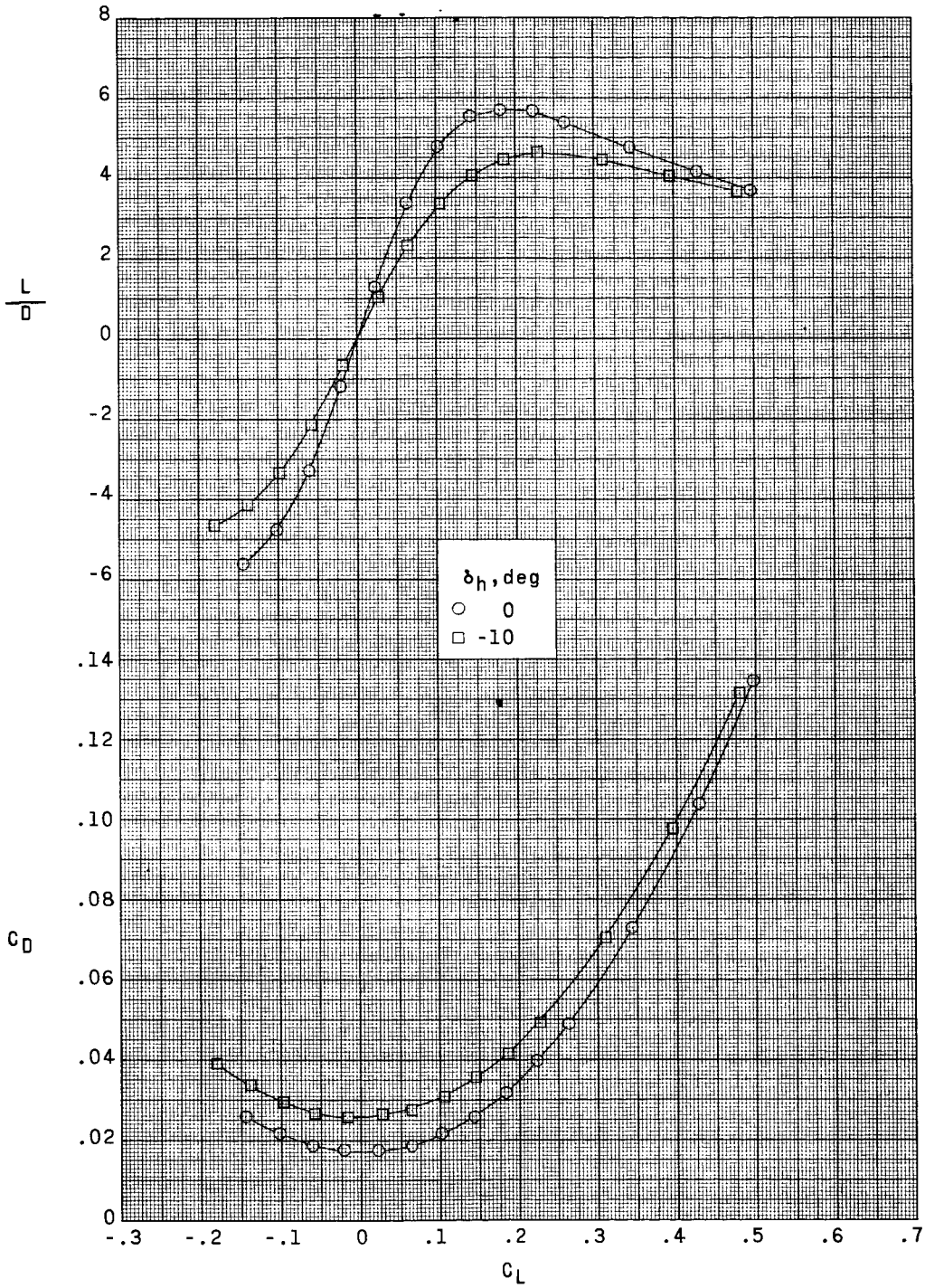

(c) Concluded.

Figure 3.- Concluded.

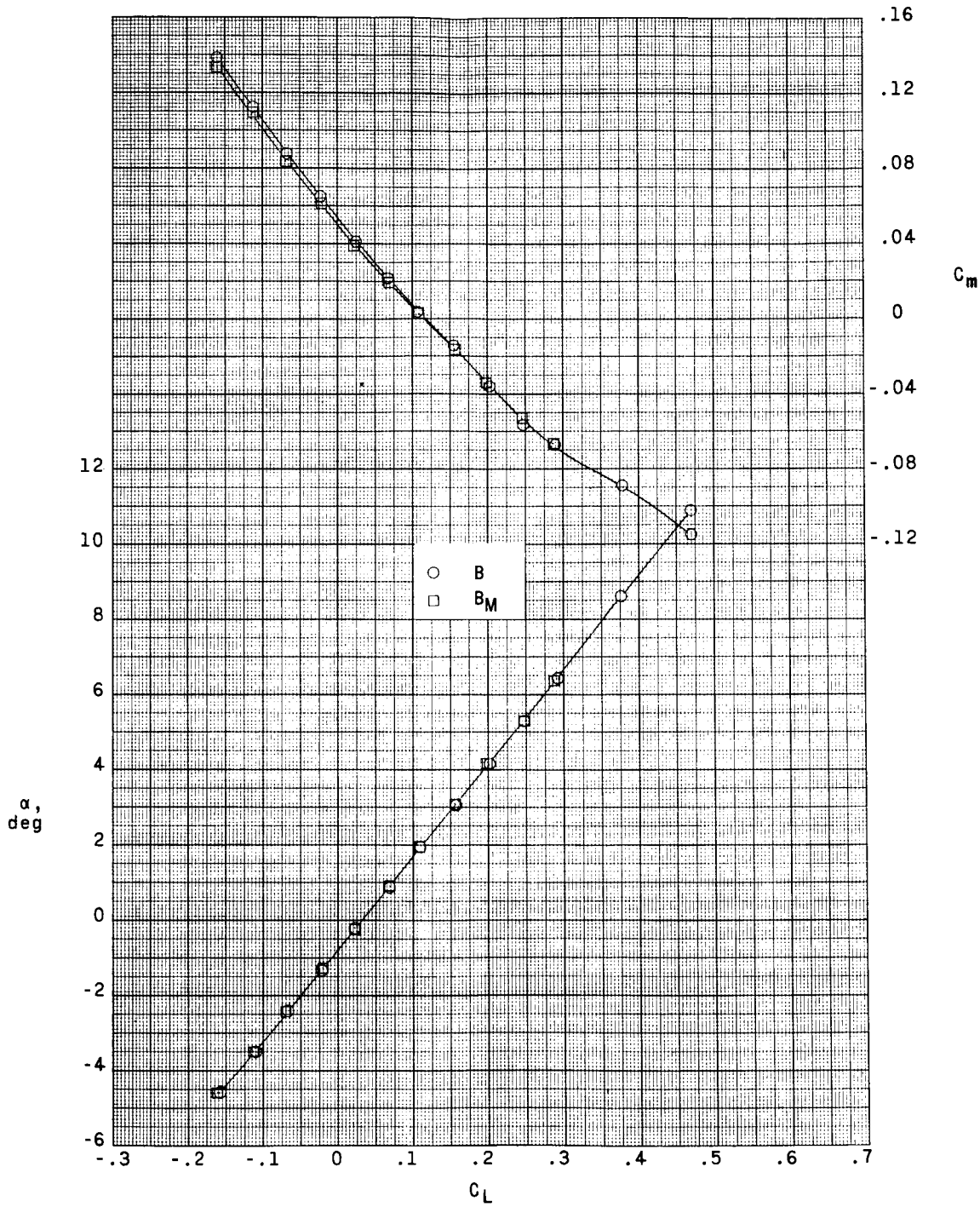

(a) M = 2.40.

Figure 4.- Effect of modified body shape on the aerodynamic characteristics in pitch for the configuration with wing glove 2. $\Lambda = 70^{\circ}$.

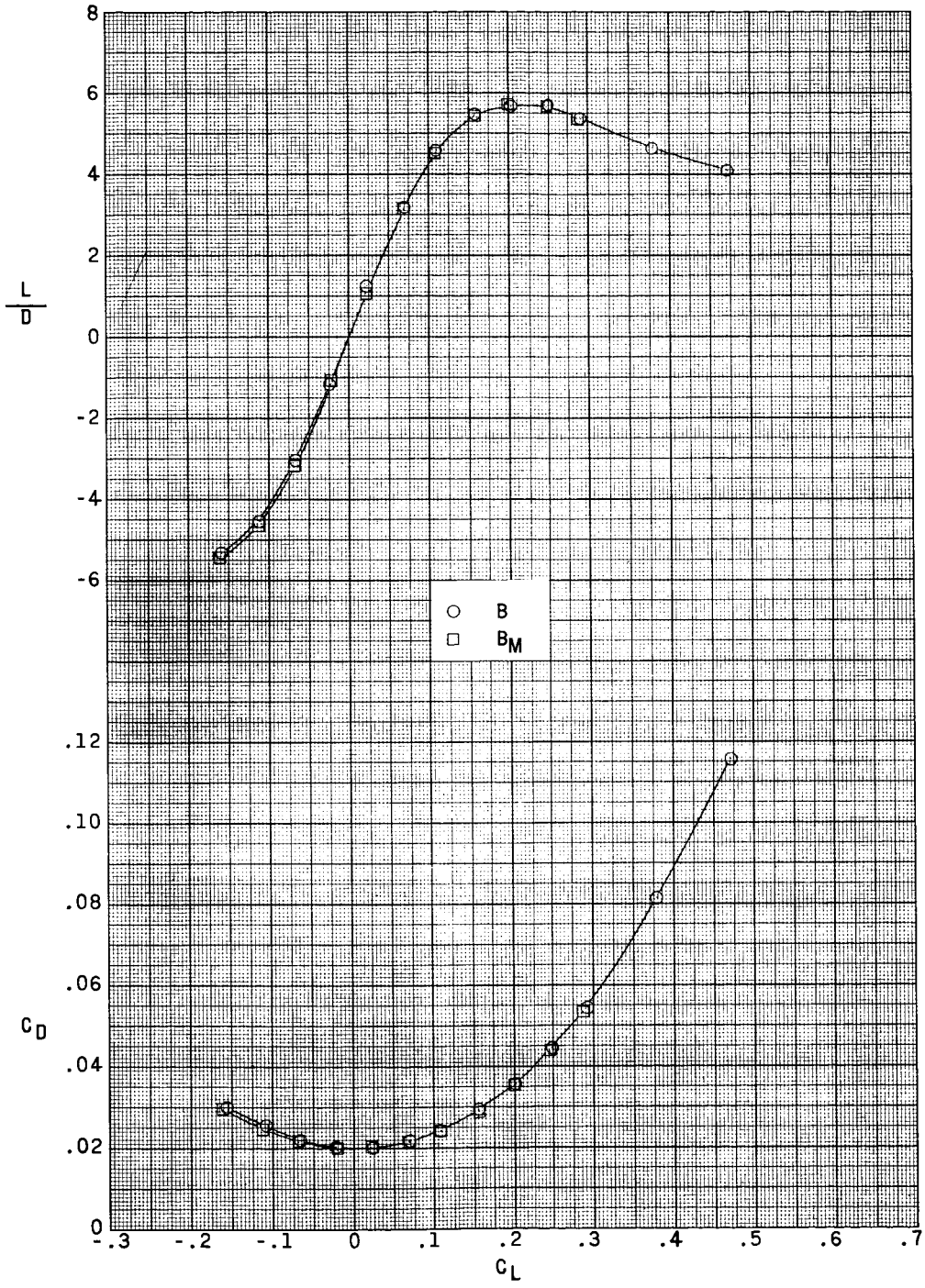

(a) Concluded.

Figure 4.- Continued.

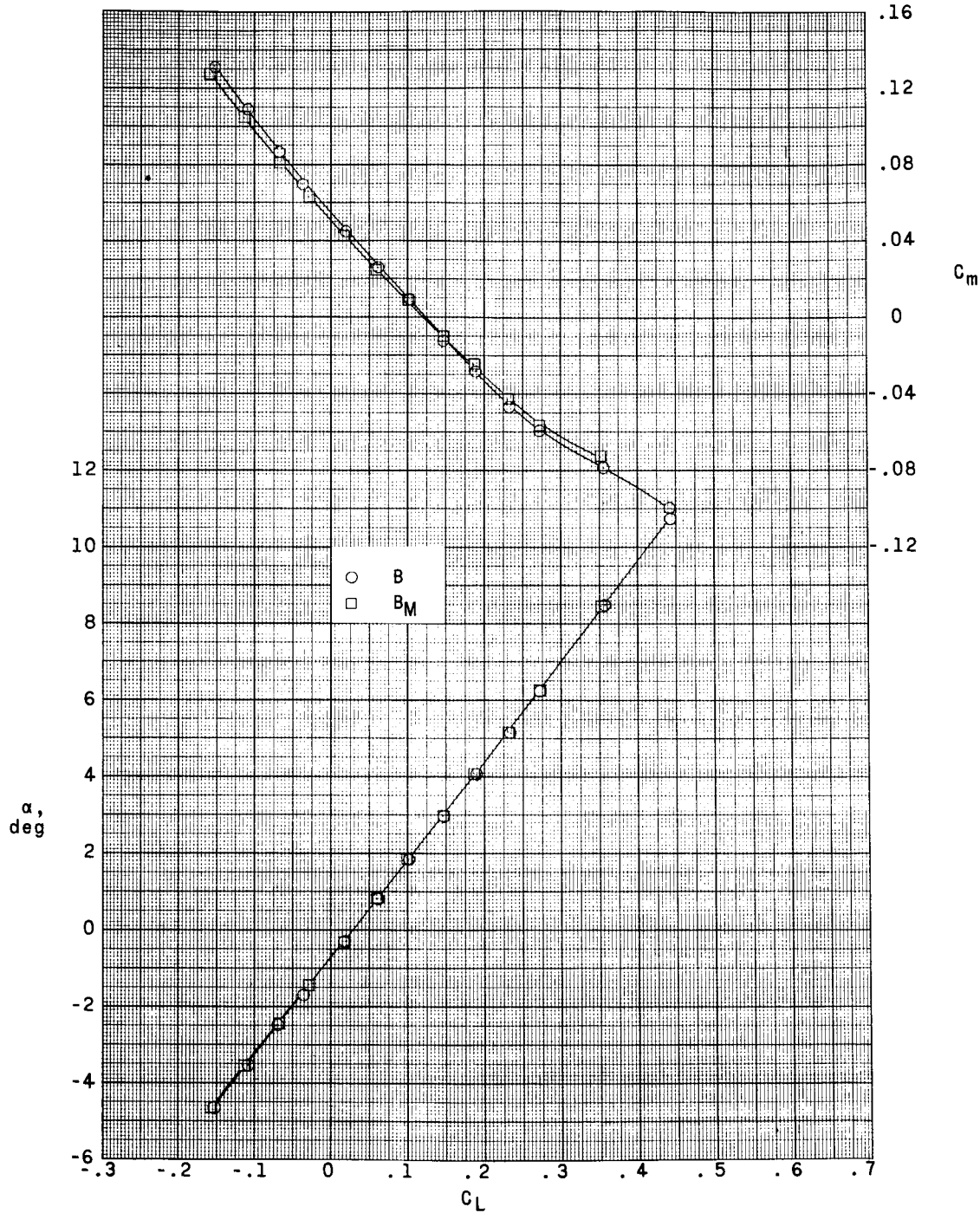

(b) M = 2.60.

Figure 4.- Continued.

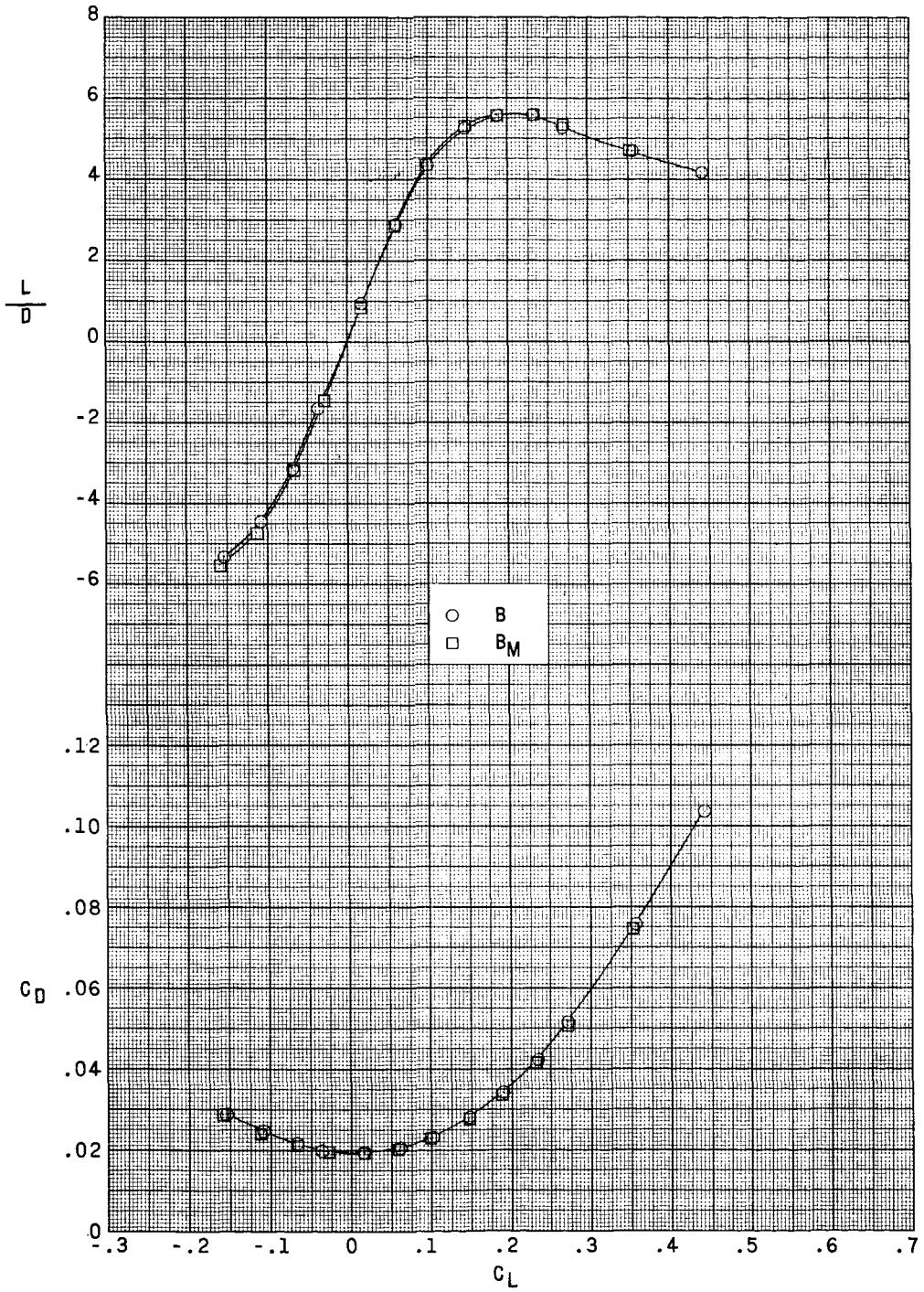

(b) Concluded.

Figure 4.- Continued.

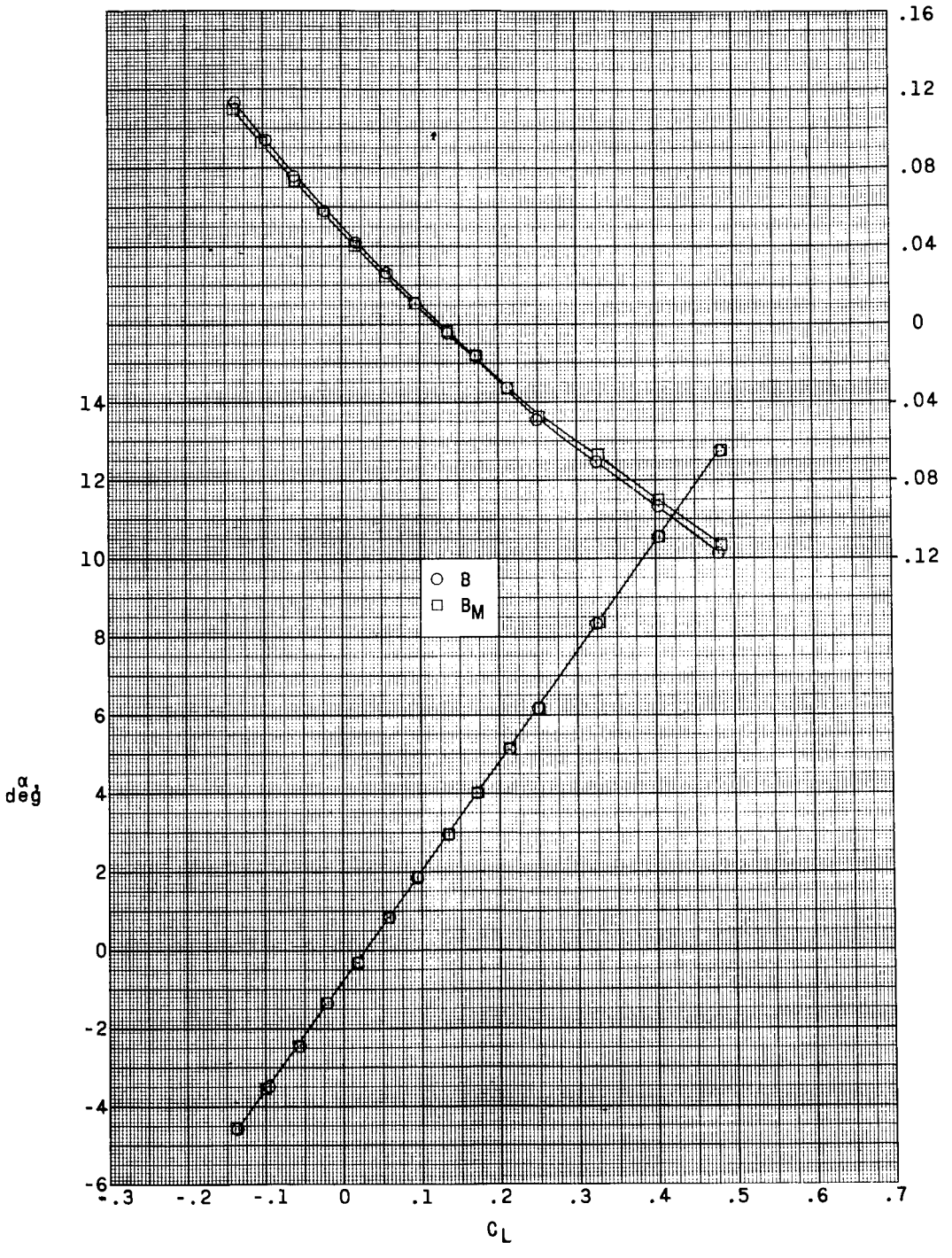

(c) M = 2.96.

Figure 4.- Continued.

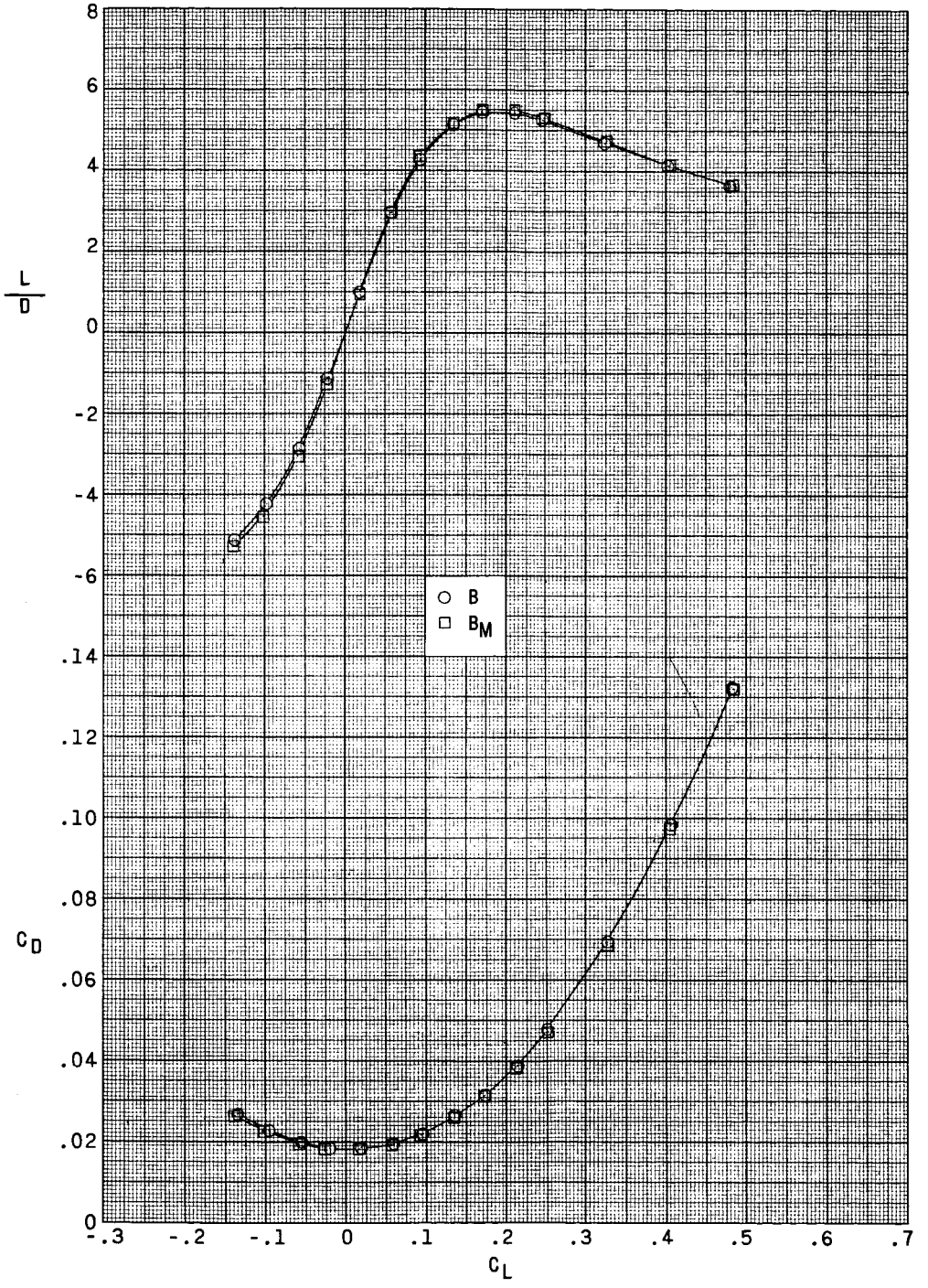

(c) Concluded.

Figure 4.- Concluded.

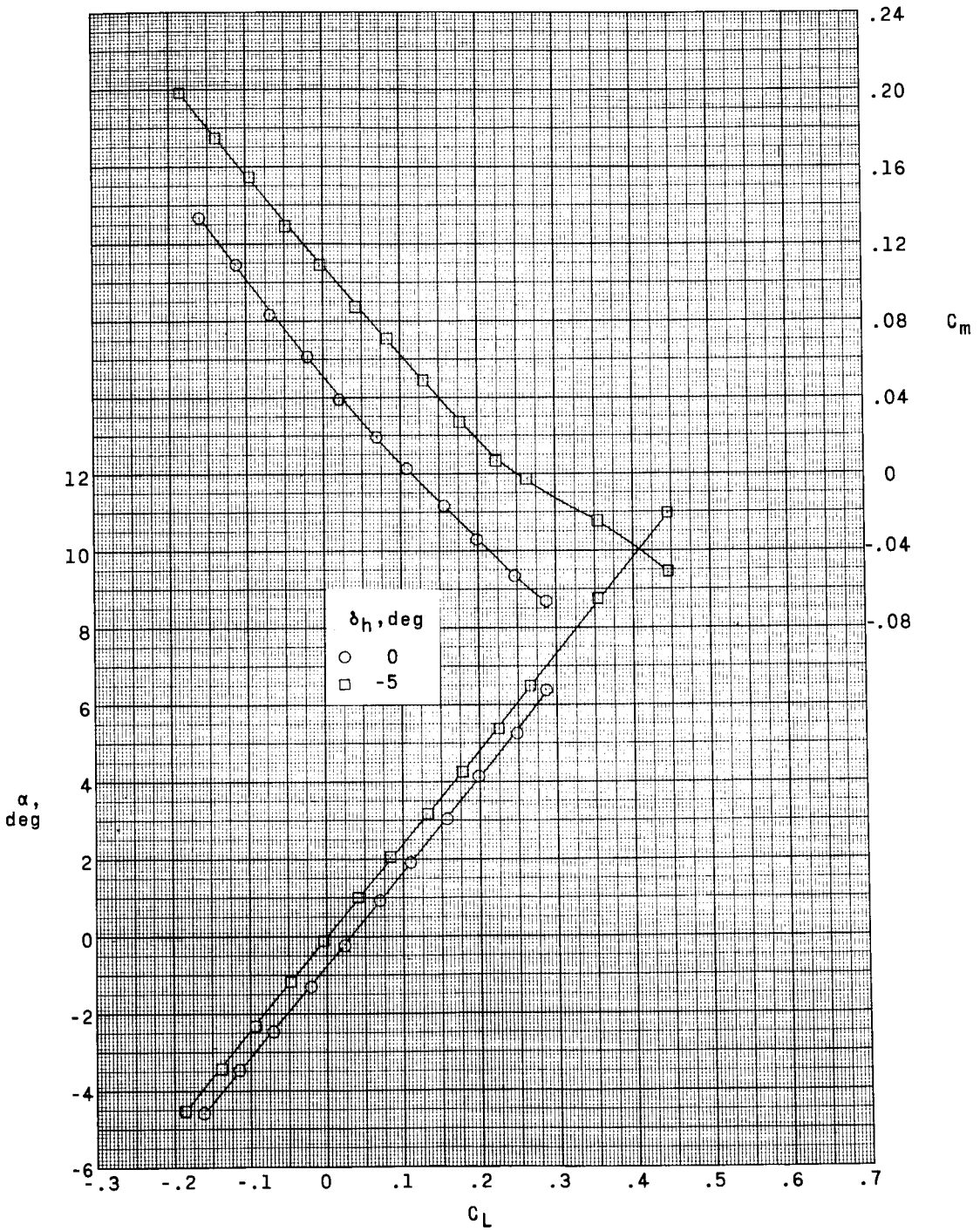

(a) M = 2.40.

Figure 5.- Effect of horizontal-tail deflection on the aerodynamic characteristics in pitch for the configuration with modified body shape and wing glove 2. $\Lambda = 70^{\circ}$.

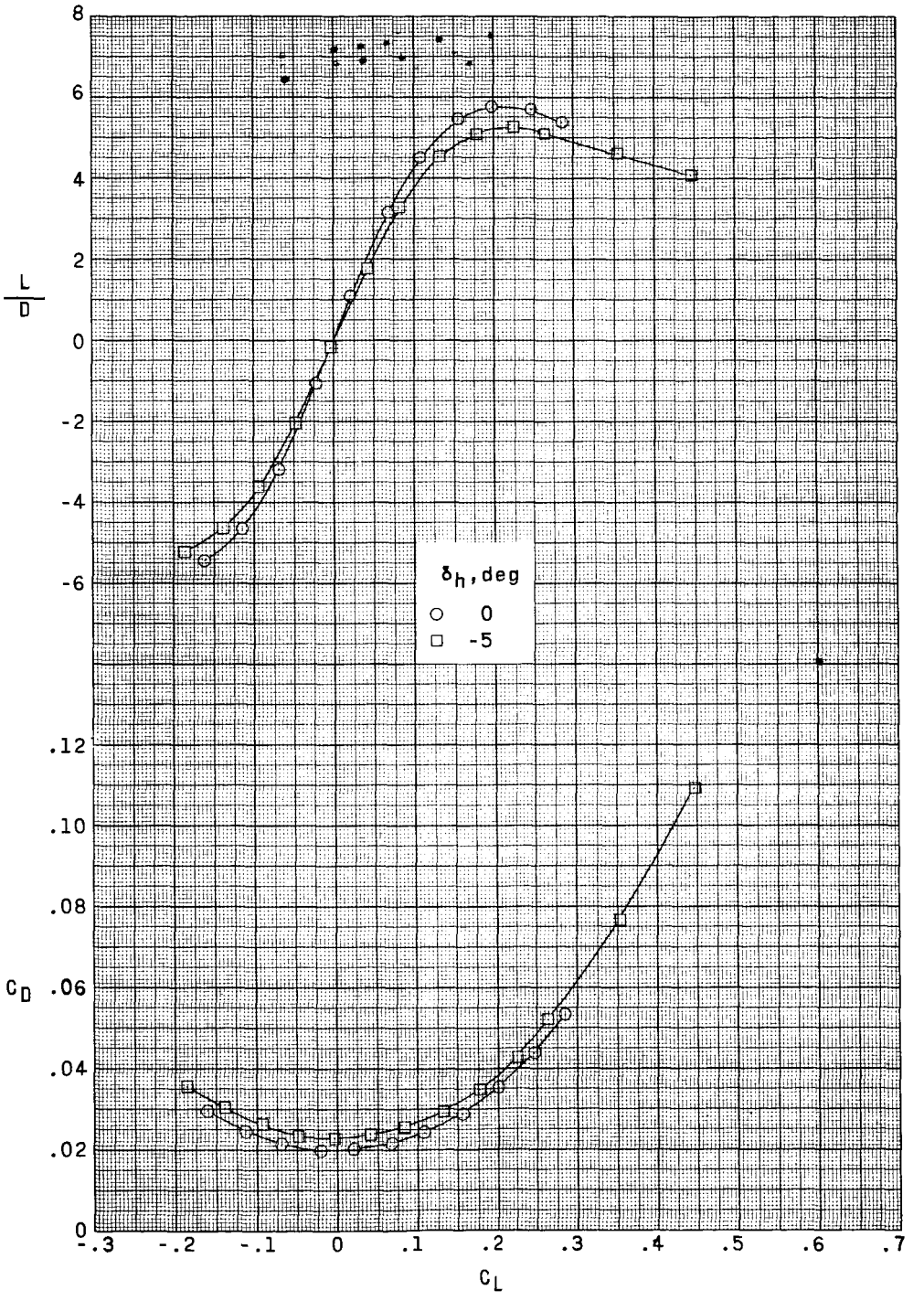

(a) Concluded.

Figure 5.- Continued.

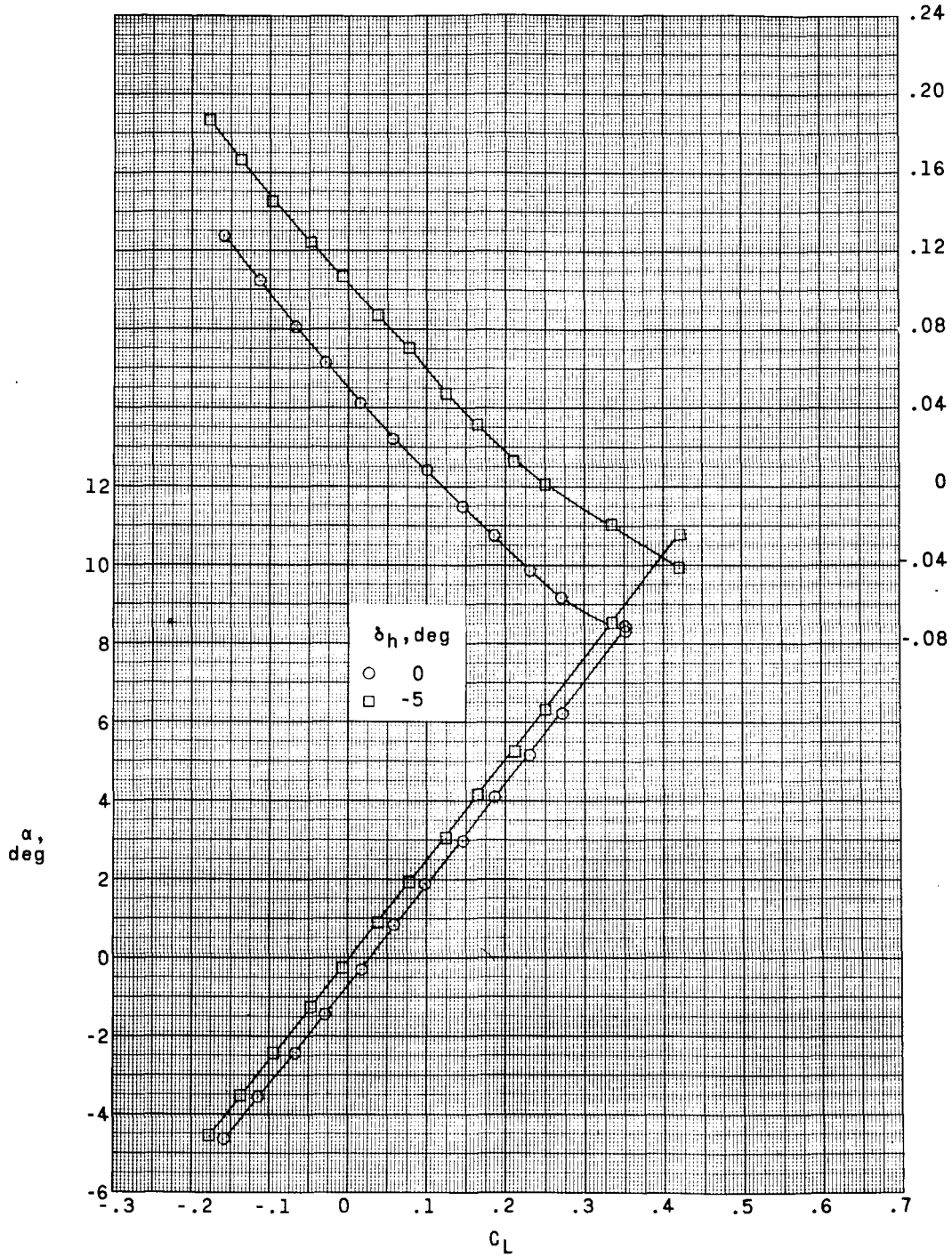

(b) M = 2.60.

Figure 5.- Continued.

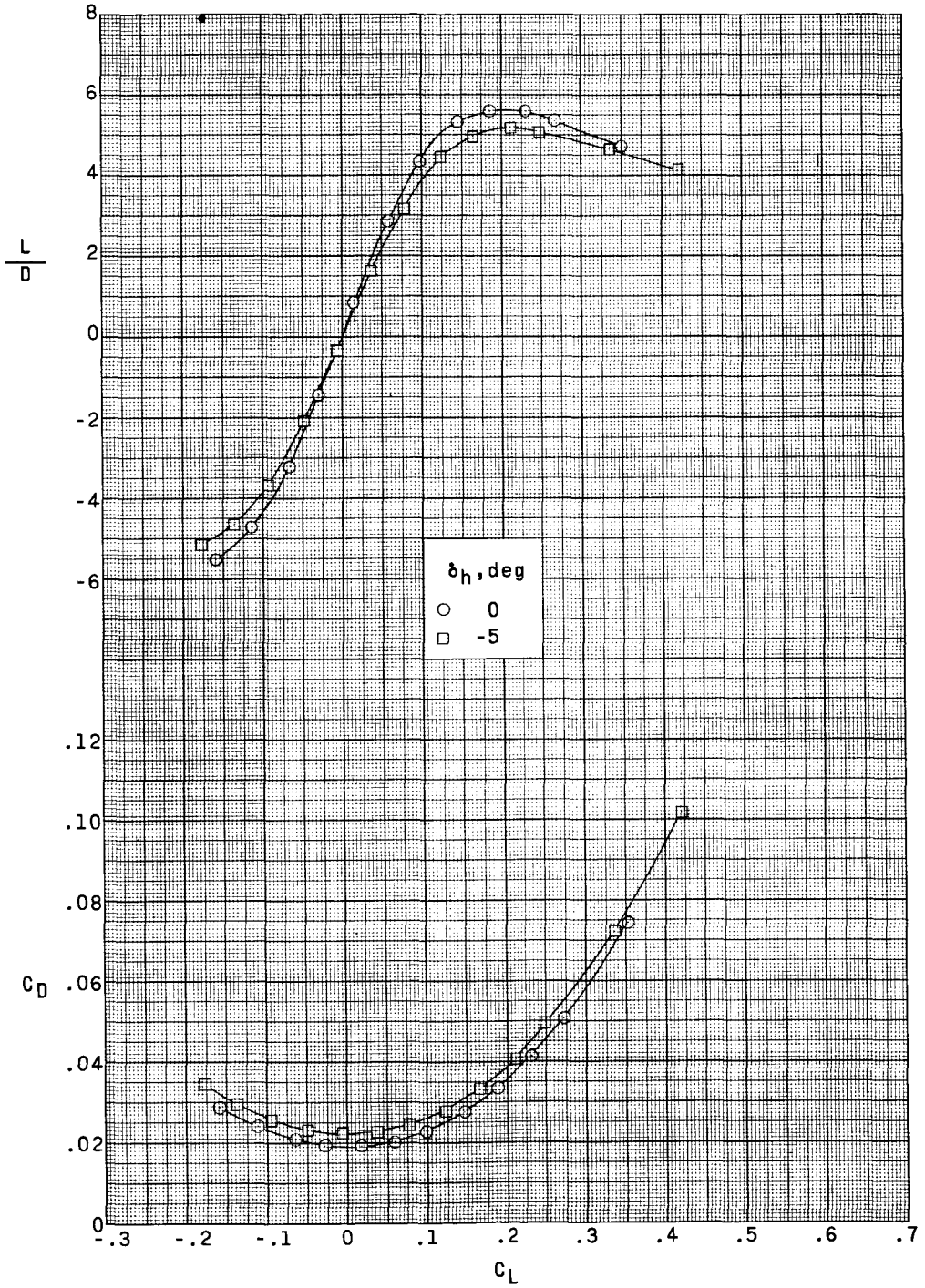

(b) Concluded.

Figure 5.- Continued.

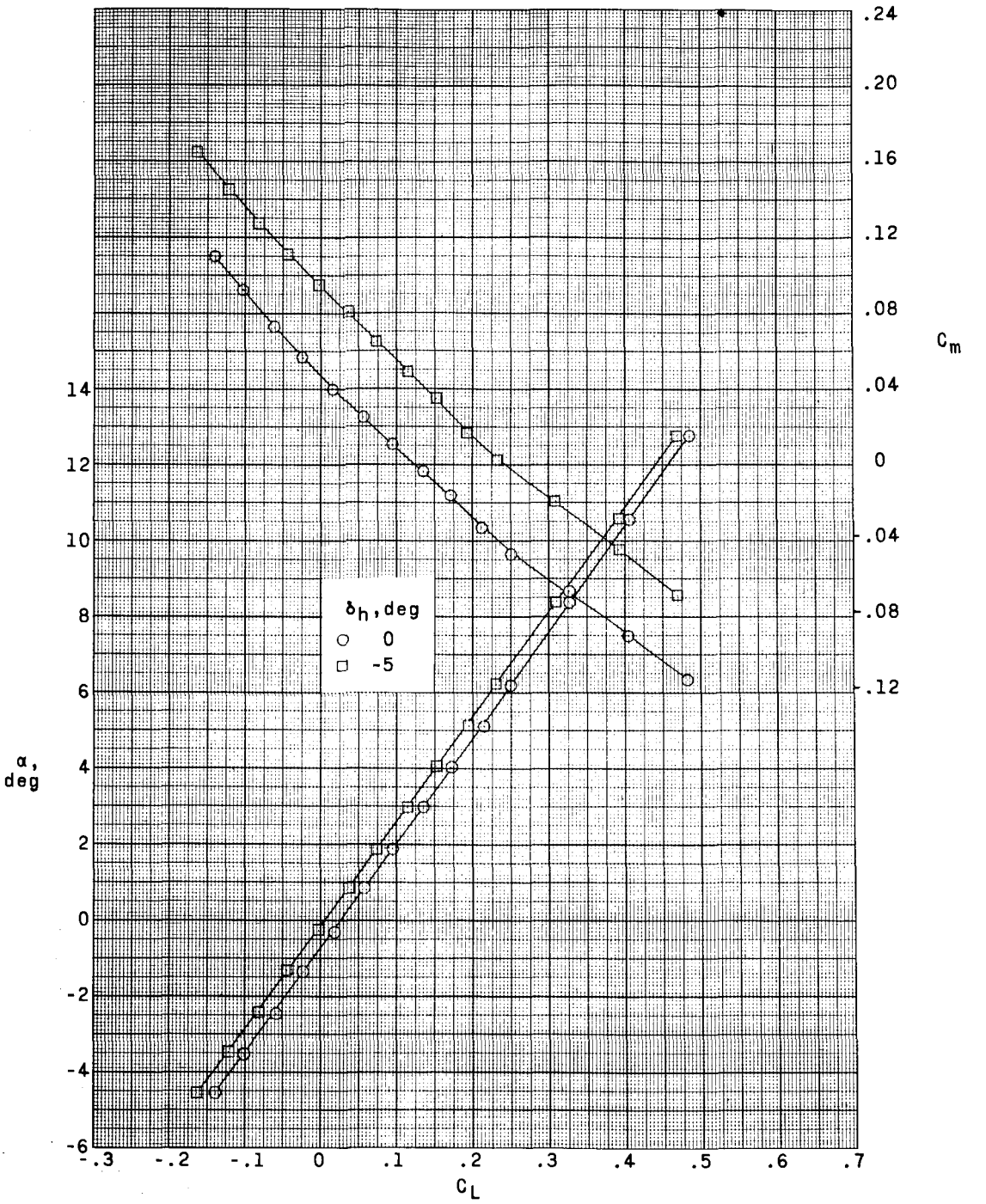

(c) M = 2.96.

Figure 5.- Continued.

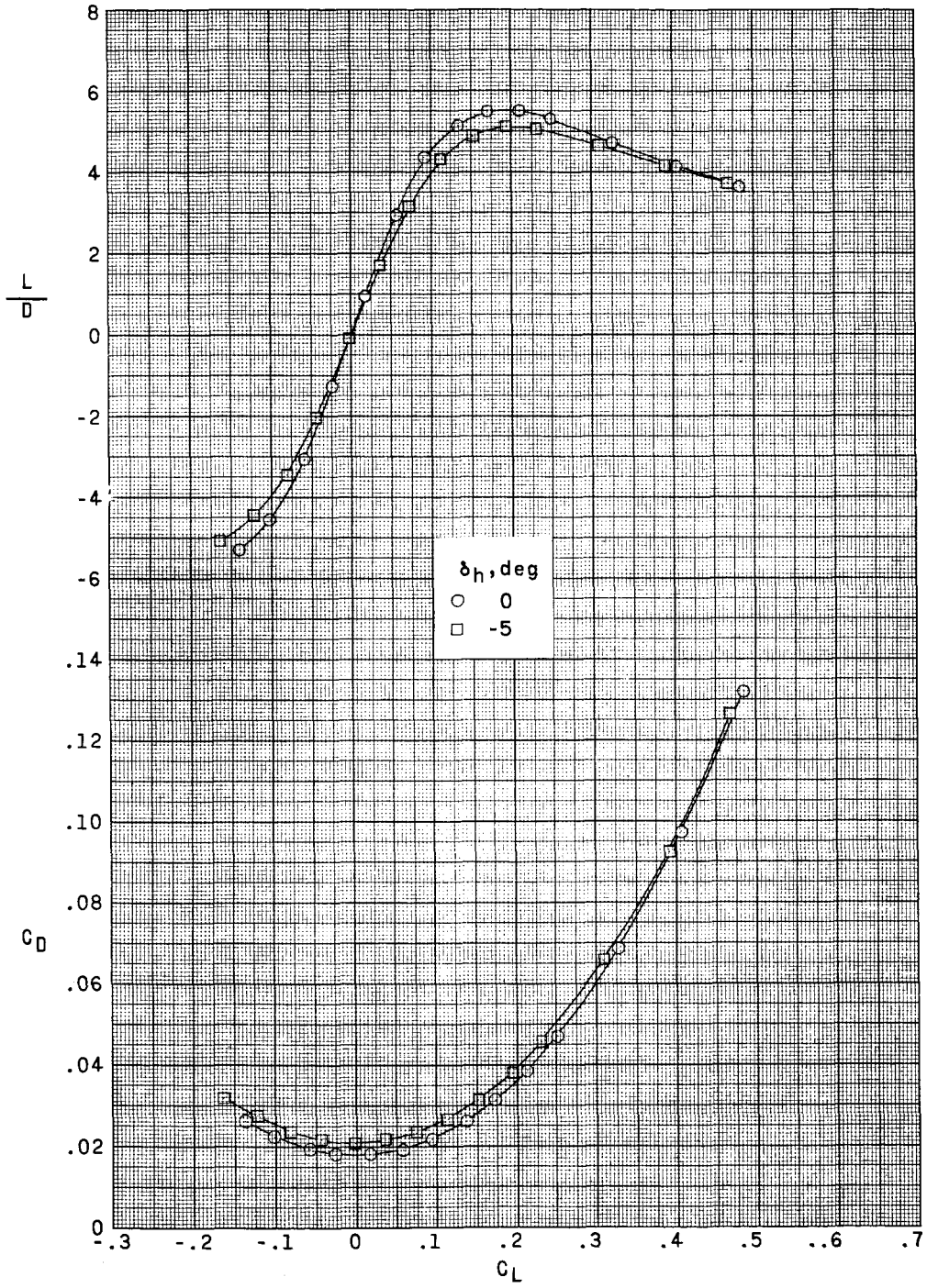

(c) Concluded.

Figure 5.- Concluded.

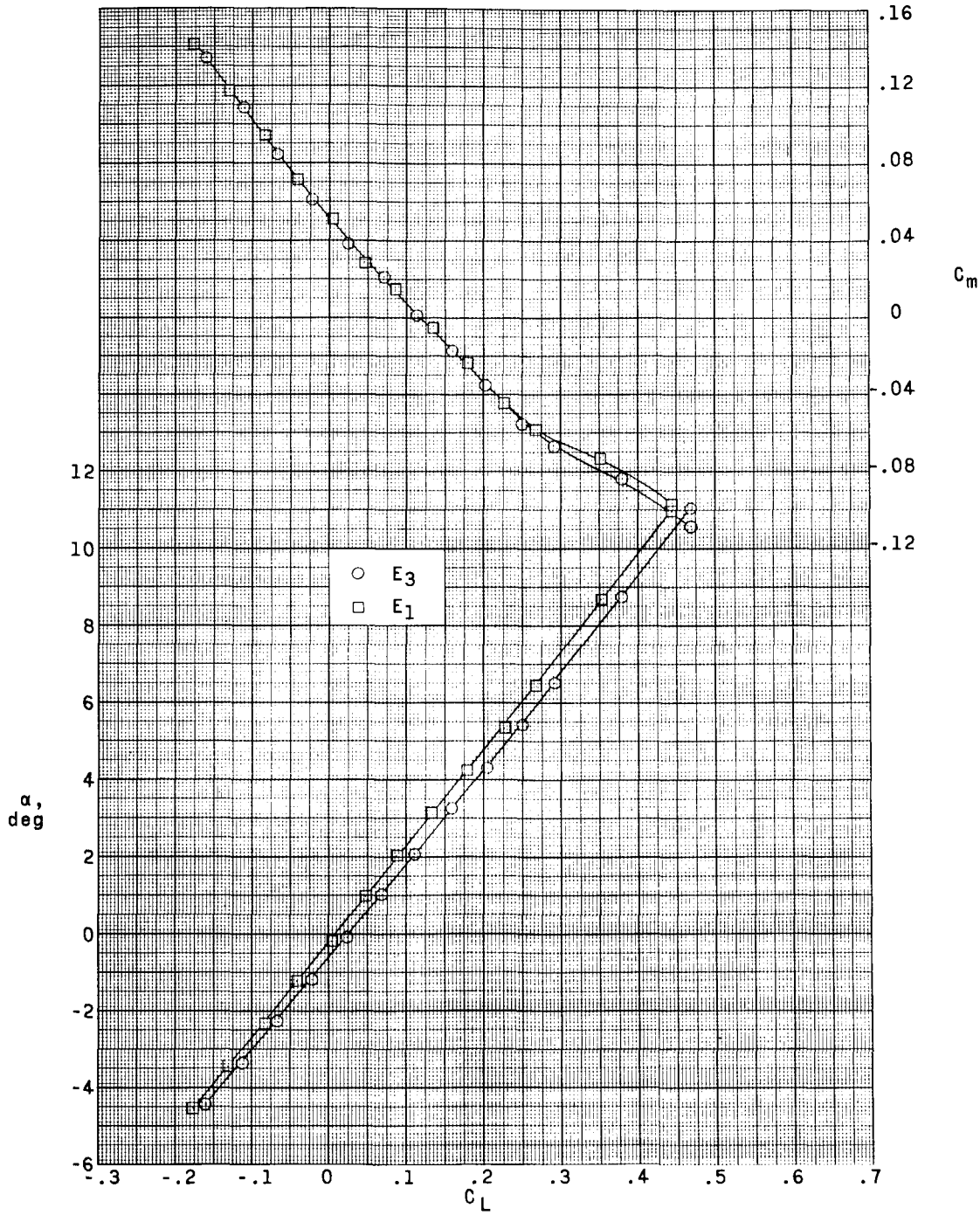

(a) M = 2.40.

Figure 6.- Effect of removing the two wing-mounted engines on the aerodynamic characteristics in pitch for the configuration with the modified body shape and wing glove 2. $\Lambda = 70^{\circ}$.

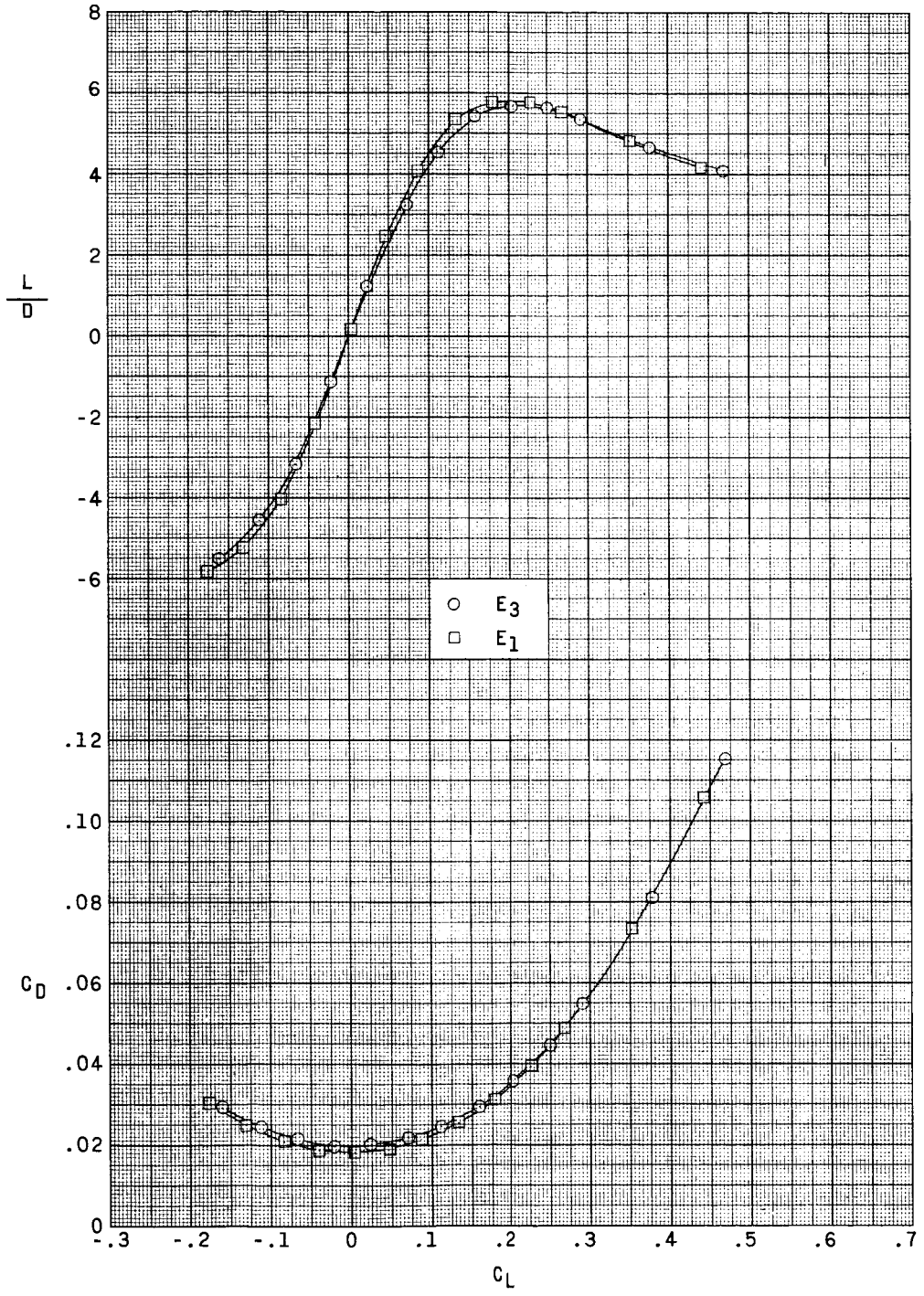

(a) Concluded.

Figure 6.- Continued.

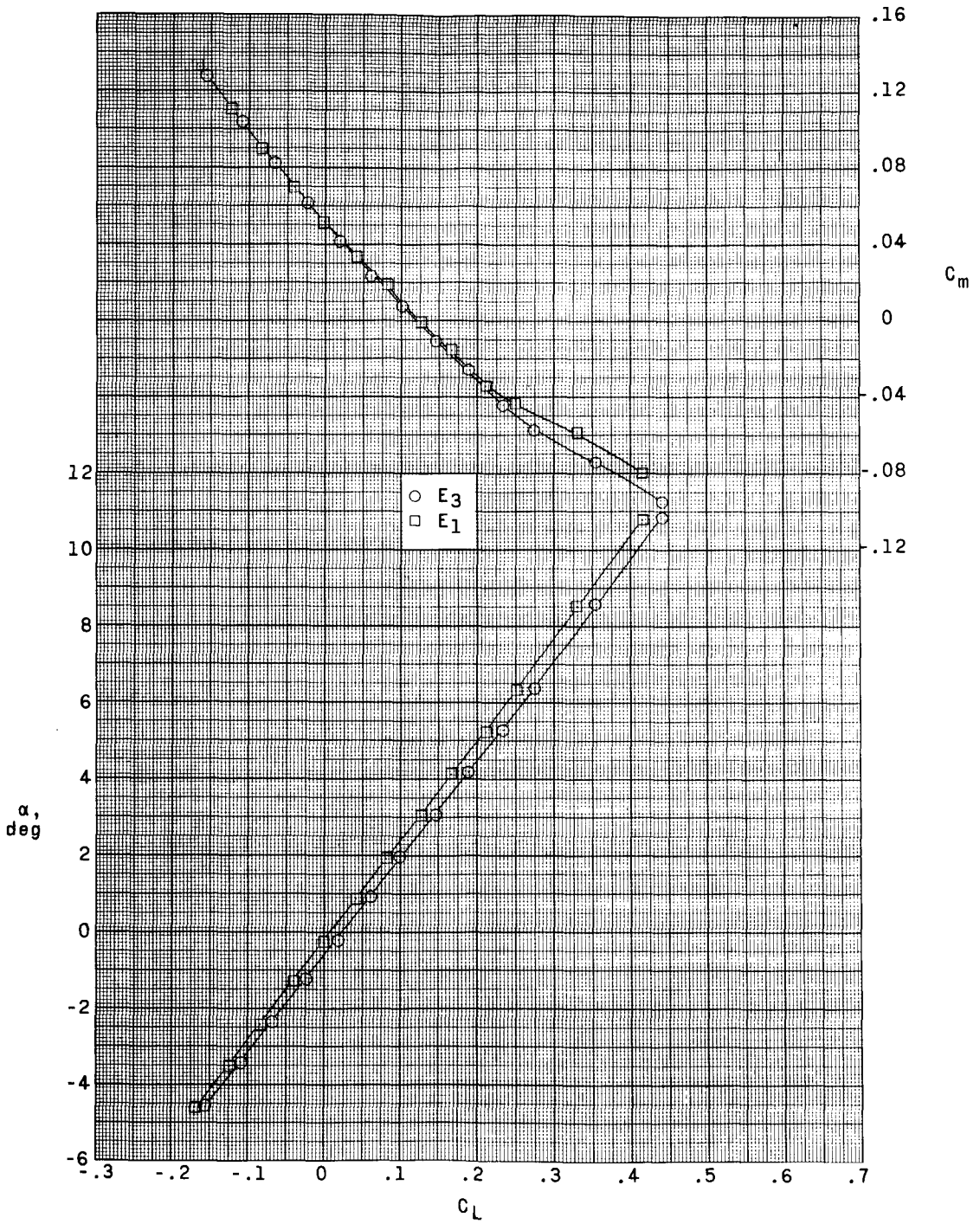

(b) M = 2.60.

Figure 6.- Continued.

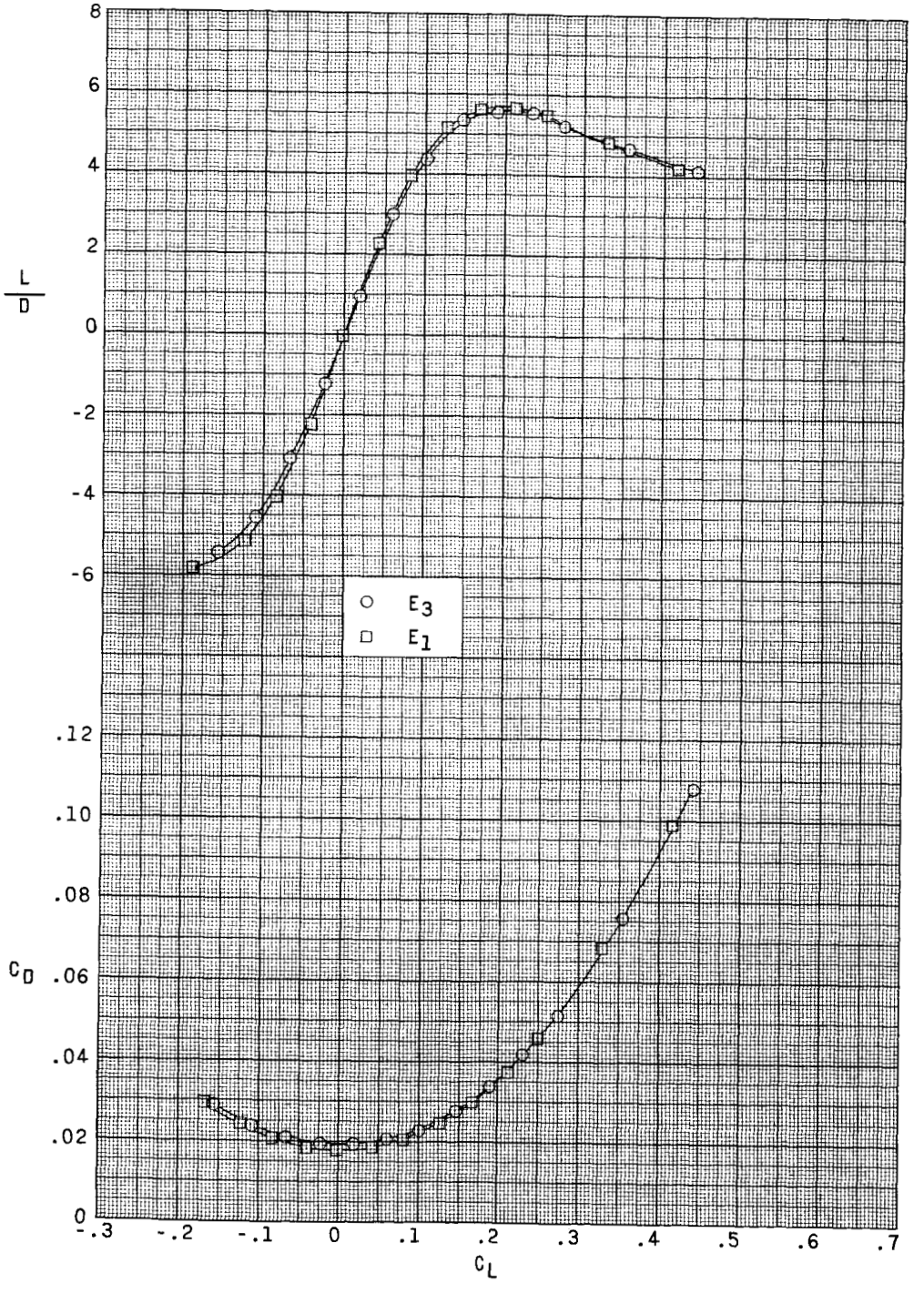

(b) Concluded.

Figure 6.- Continued.

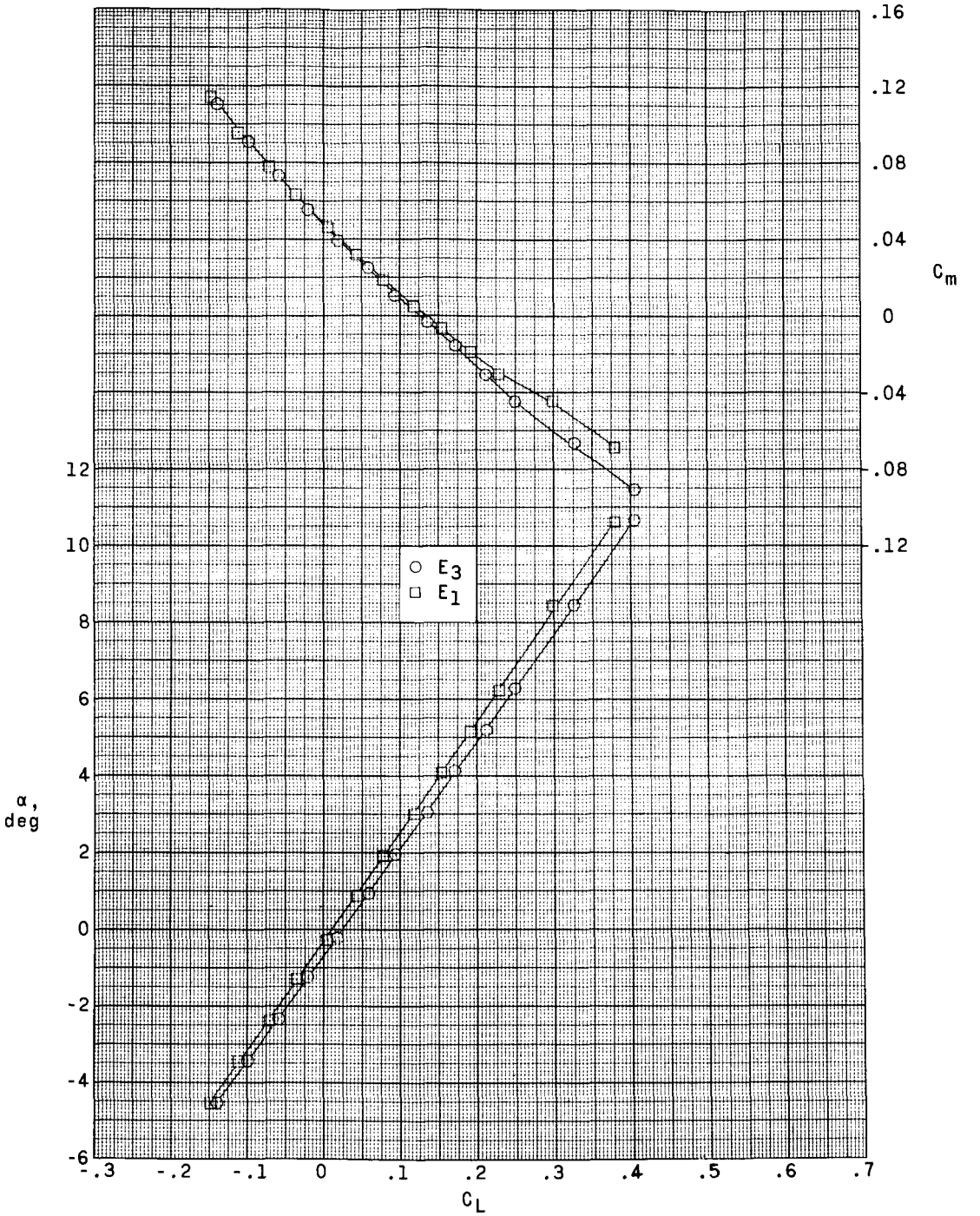

(c) M = 2.96.

Figure 6.- Continued.

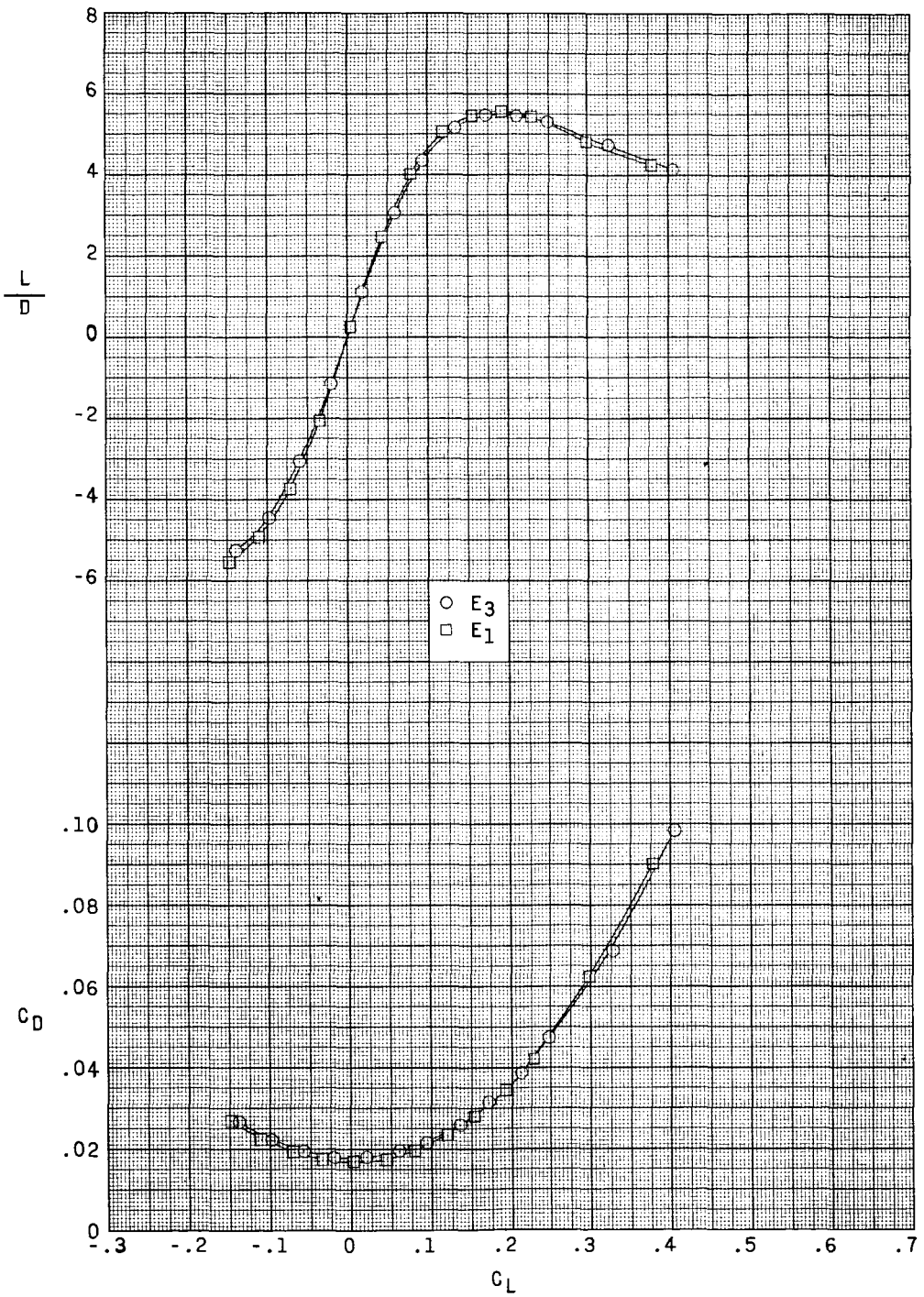

(c) Concluded.

Figure 6.- Concluded.

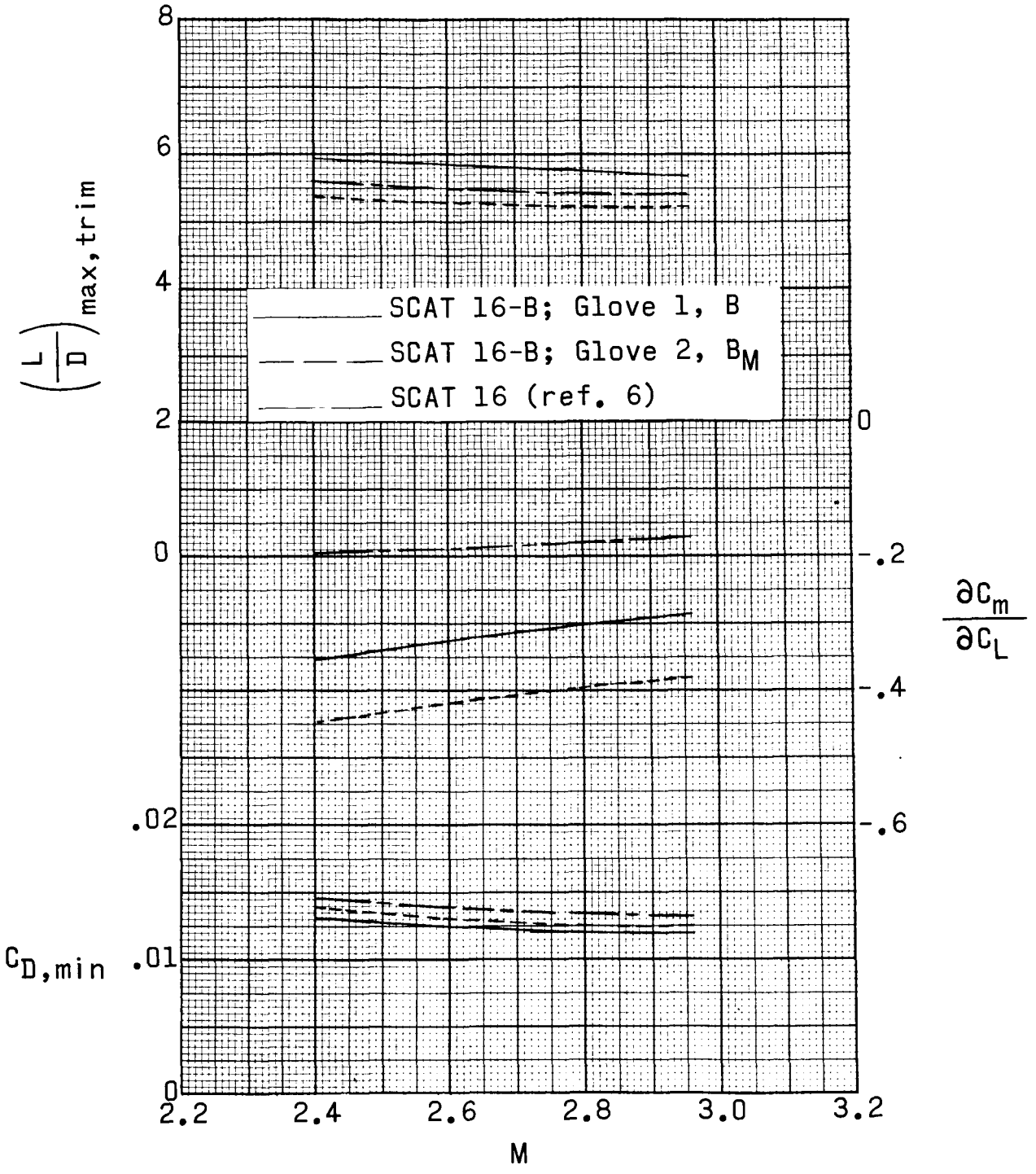

Figure 7.- Variation of the longitudinal parameters with Mach number of present configuration compared with that for the original SCAT 16 configuration (ref. 6). $\Lambda = 76^{\circ}$.

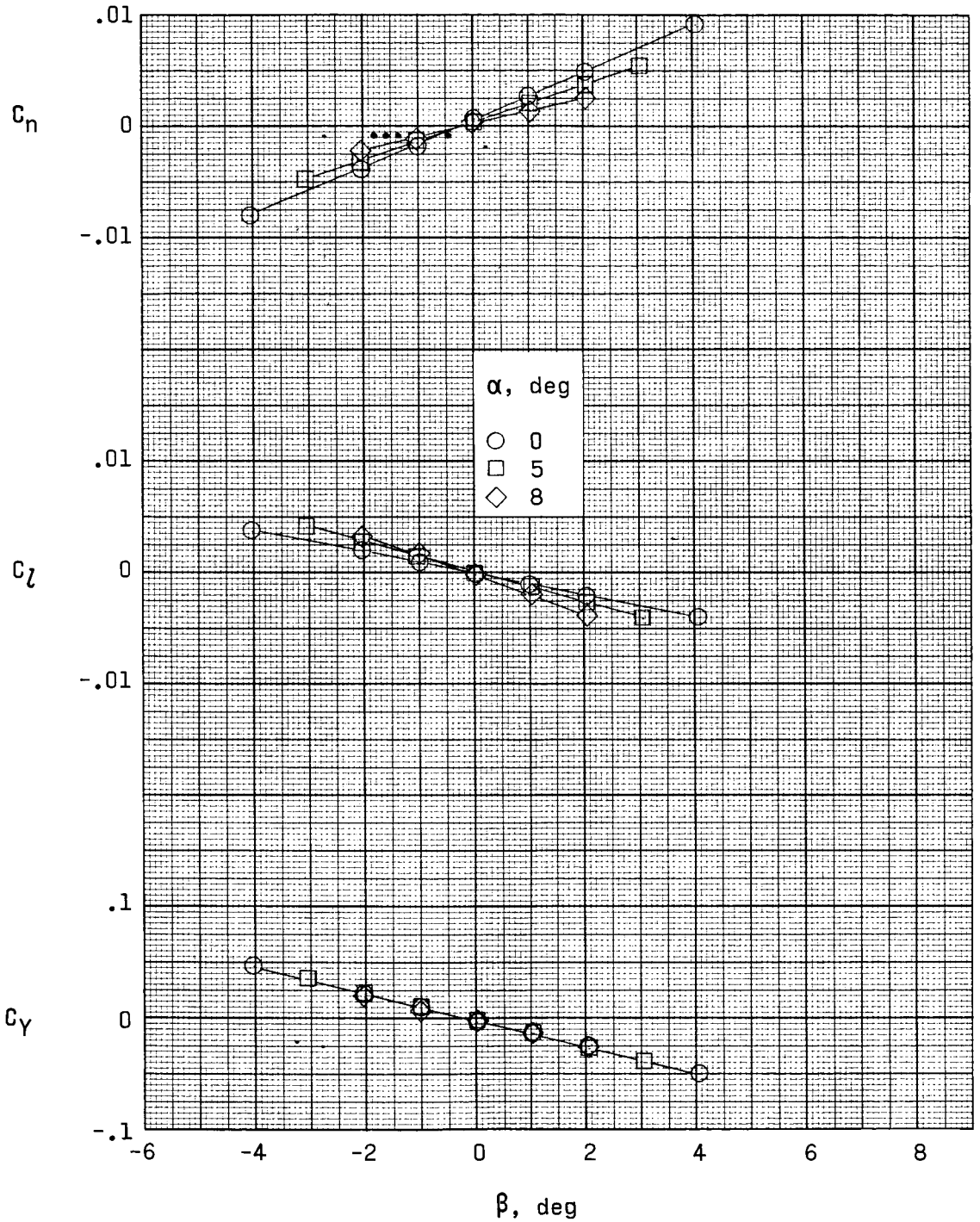

(a) M = 2.40.

Figure 8.- Aerodynamic characteristics in sideslip for the configuration with modified body shape and wing glove 2. $\Lambda = 70^{o}$.

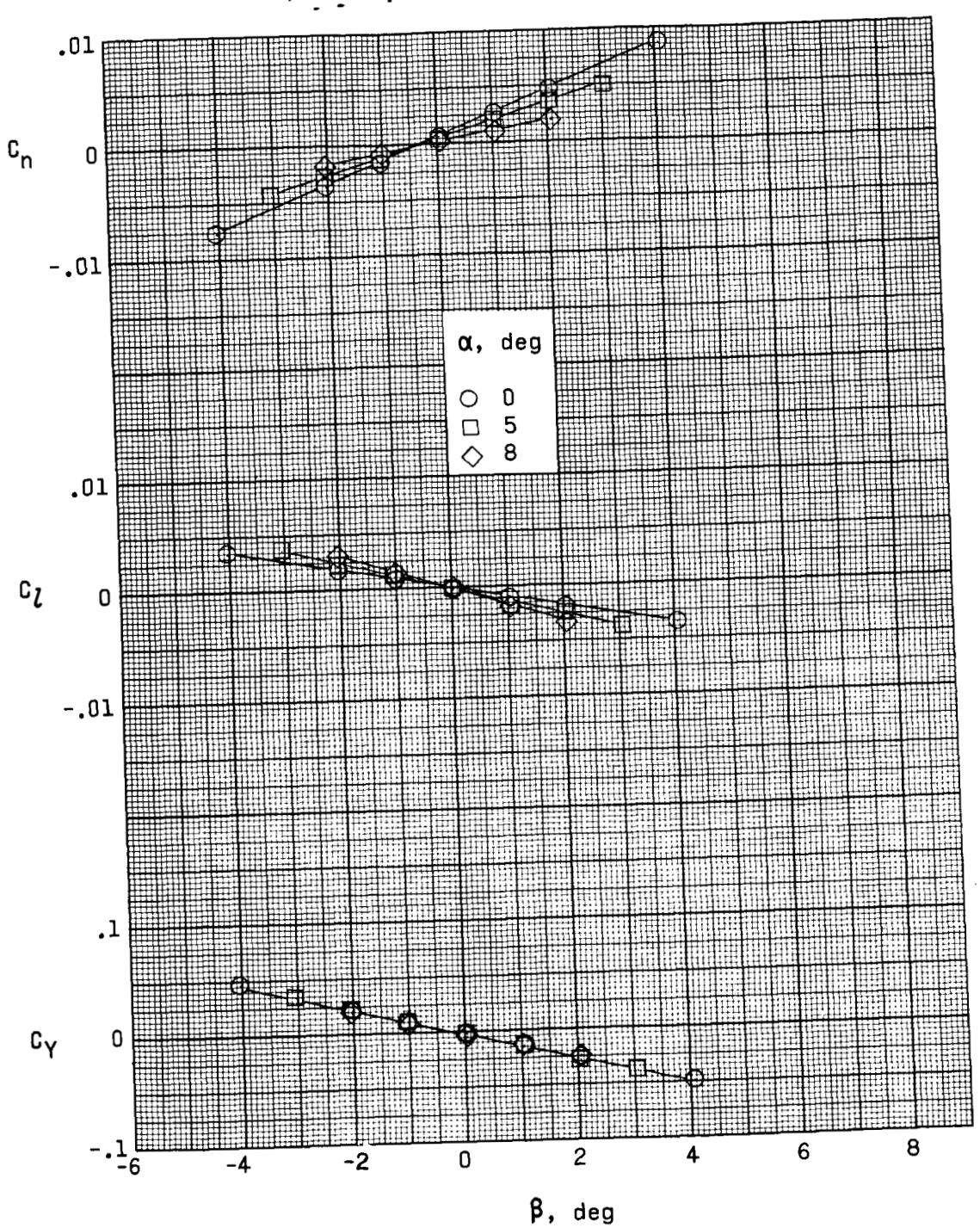

(b) M = 2.60.

Figure 8.- Continued.

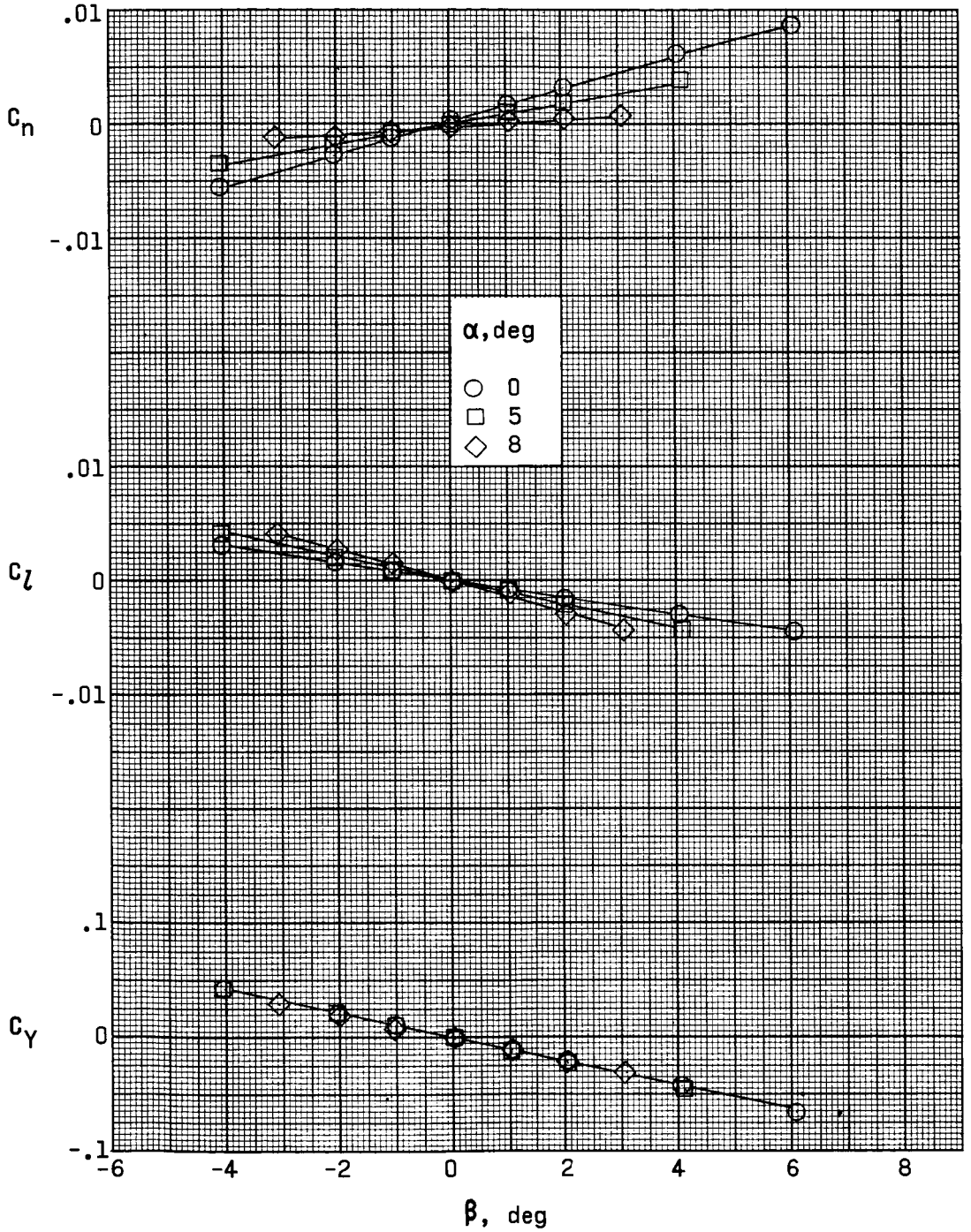

(c) M = 2.96.

Figure 8.- Concluded.

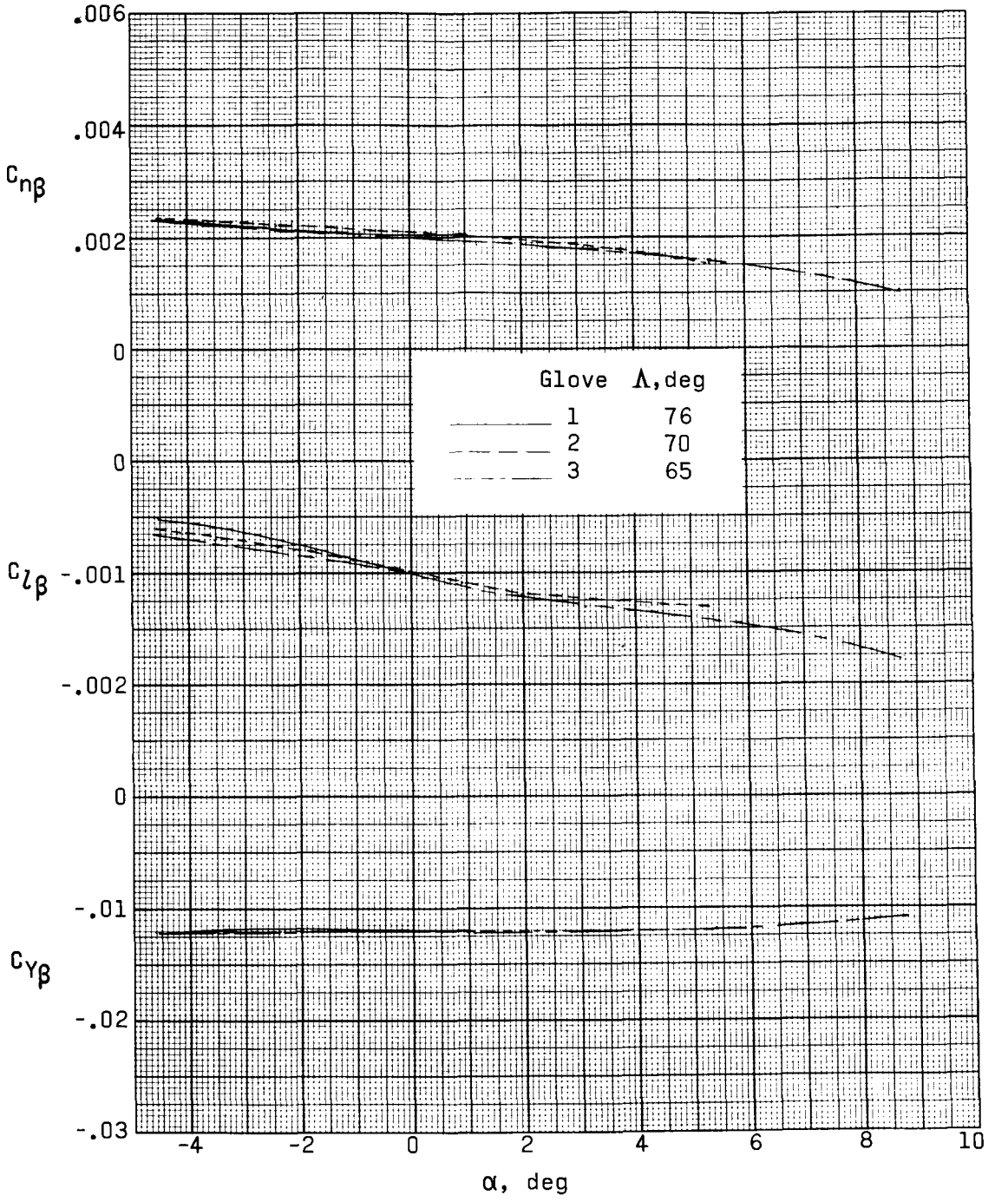

(a) M = 2.40.

Figure 9.- Effect of wing glove shape on the sideslip derivatives for the configuration with the original body shape.

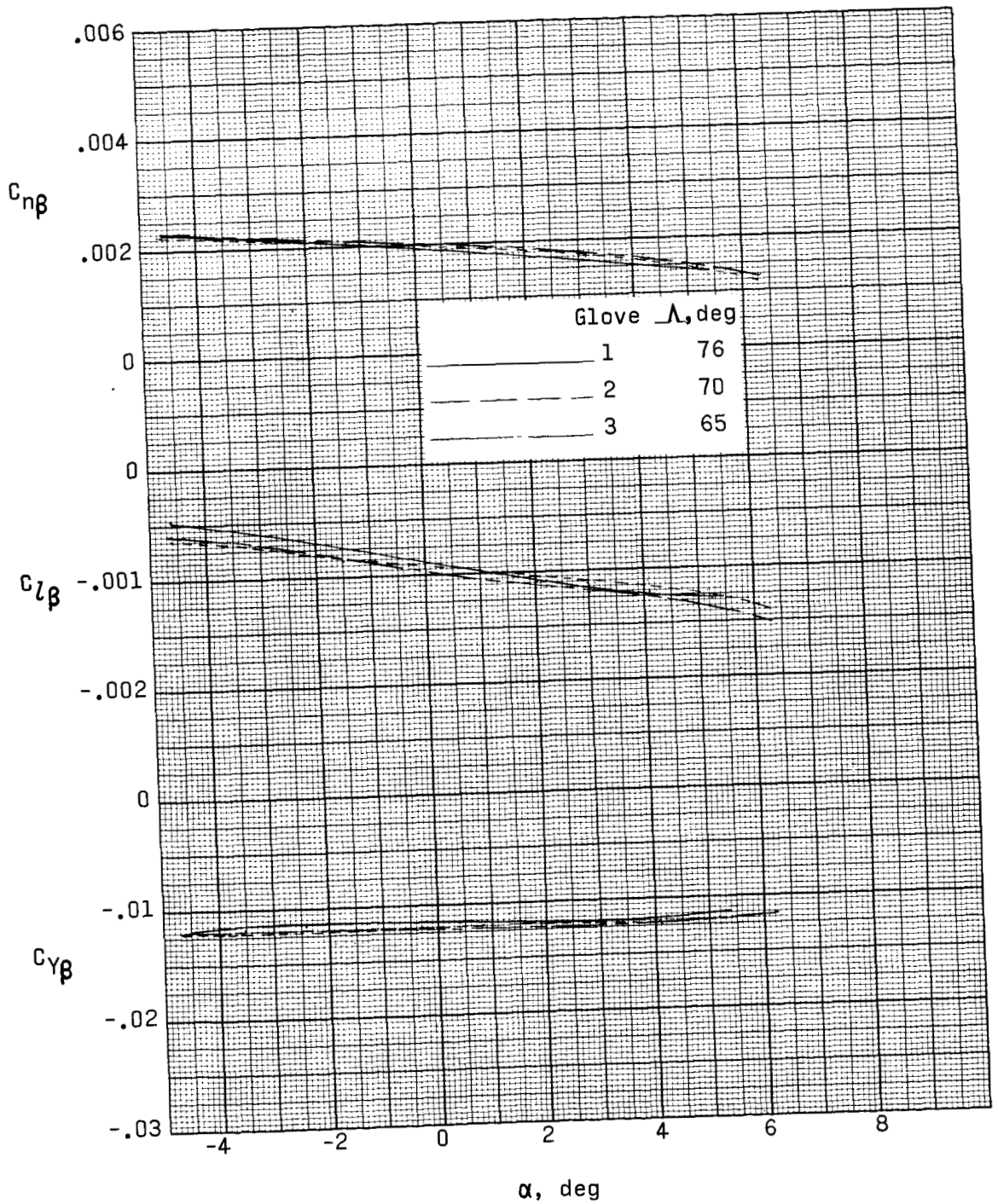

(b) M = 2.60.

Figure 9.- Continued.

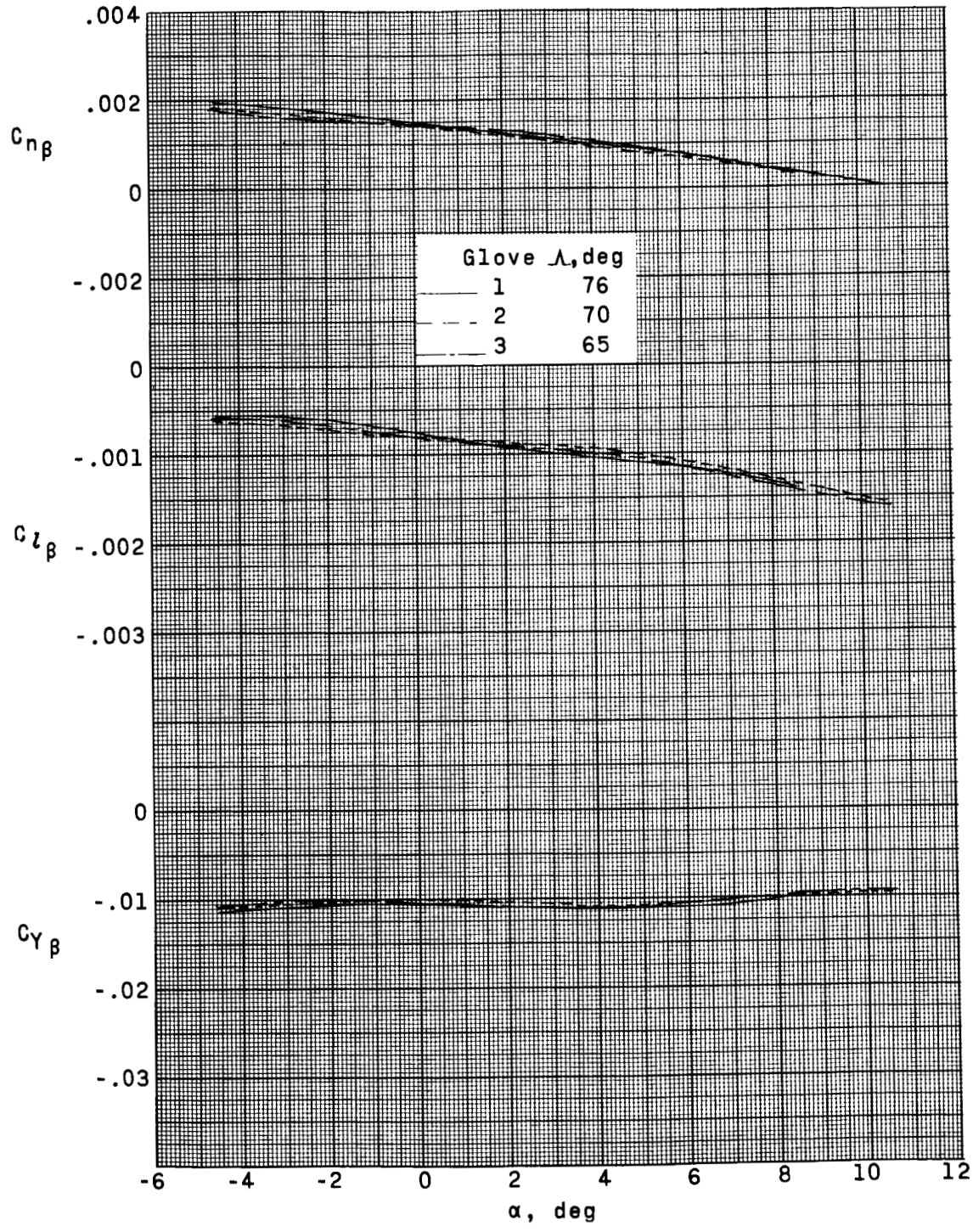

(c) M = 2.96.

Figure 9.- Concluded.

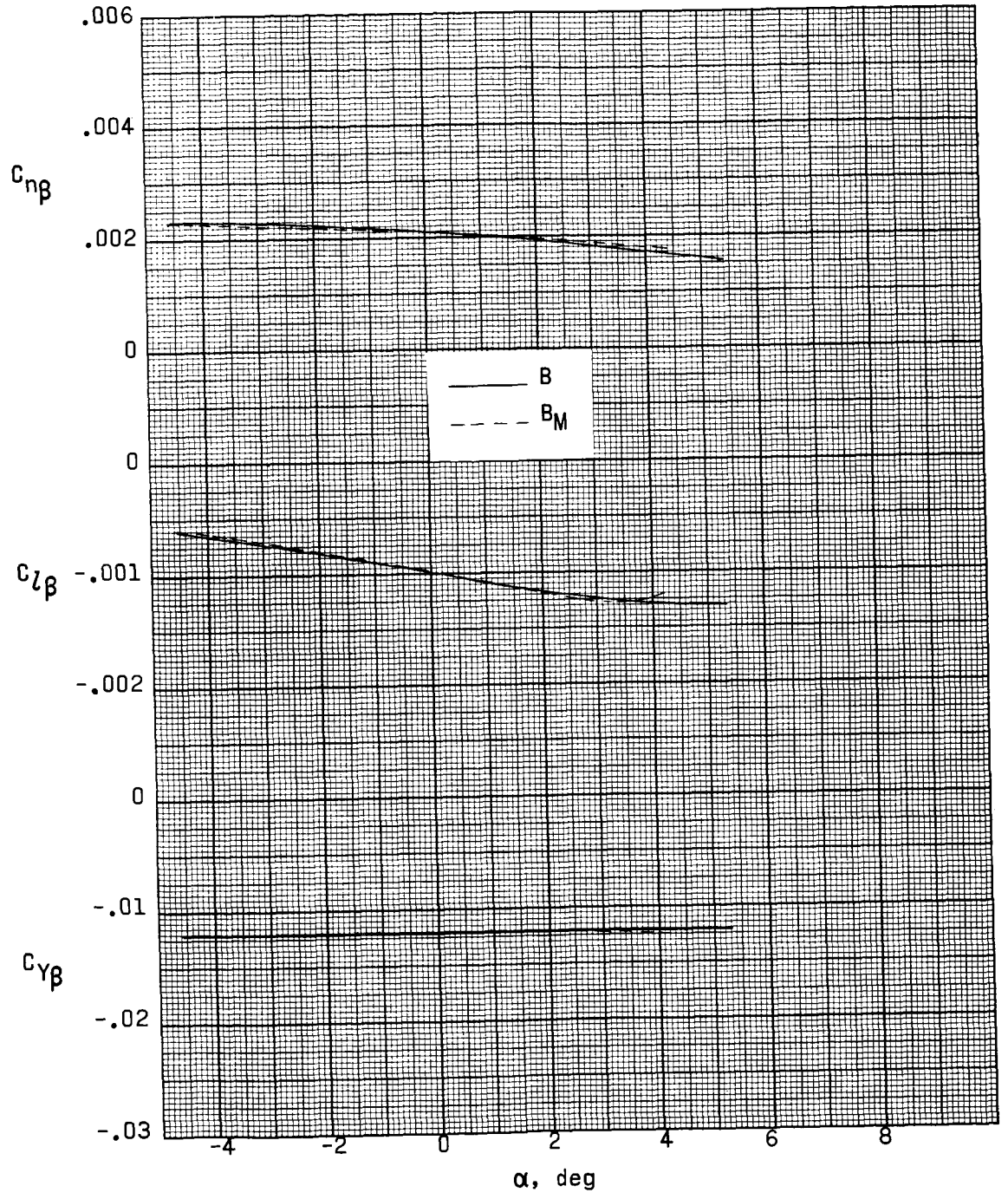

(a) M = 2.40.

Figure 10.- Effect of modified body shape on the sideslip derivatives for the configuration with wing glove 2. $\Lambda = 70^{\circ}$.

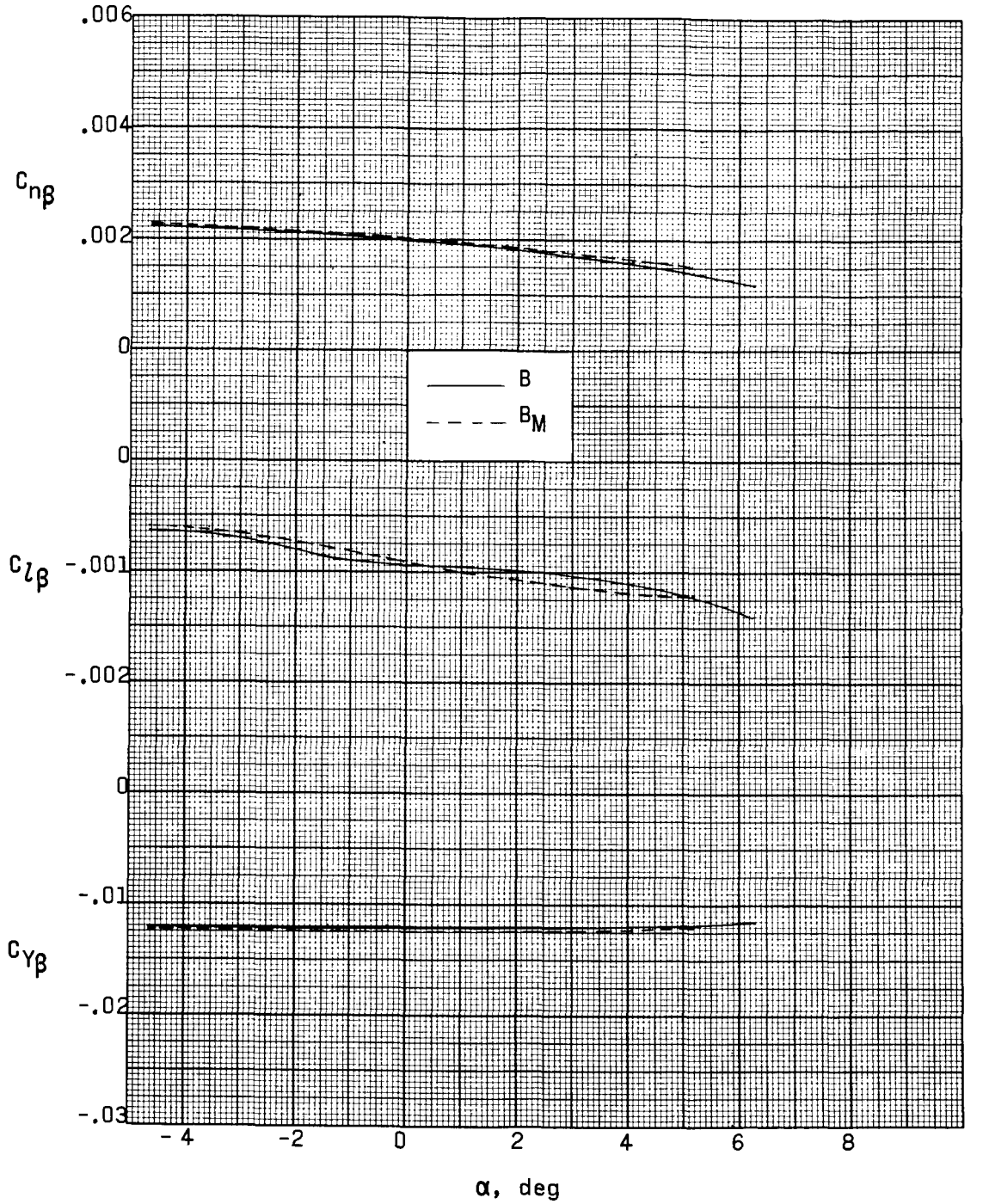

(b) M = 2.60.

Figure 10.- Continued.

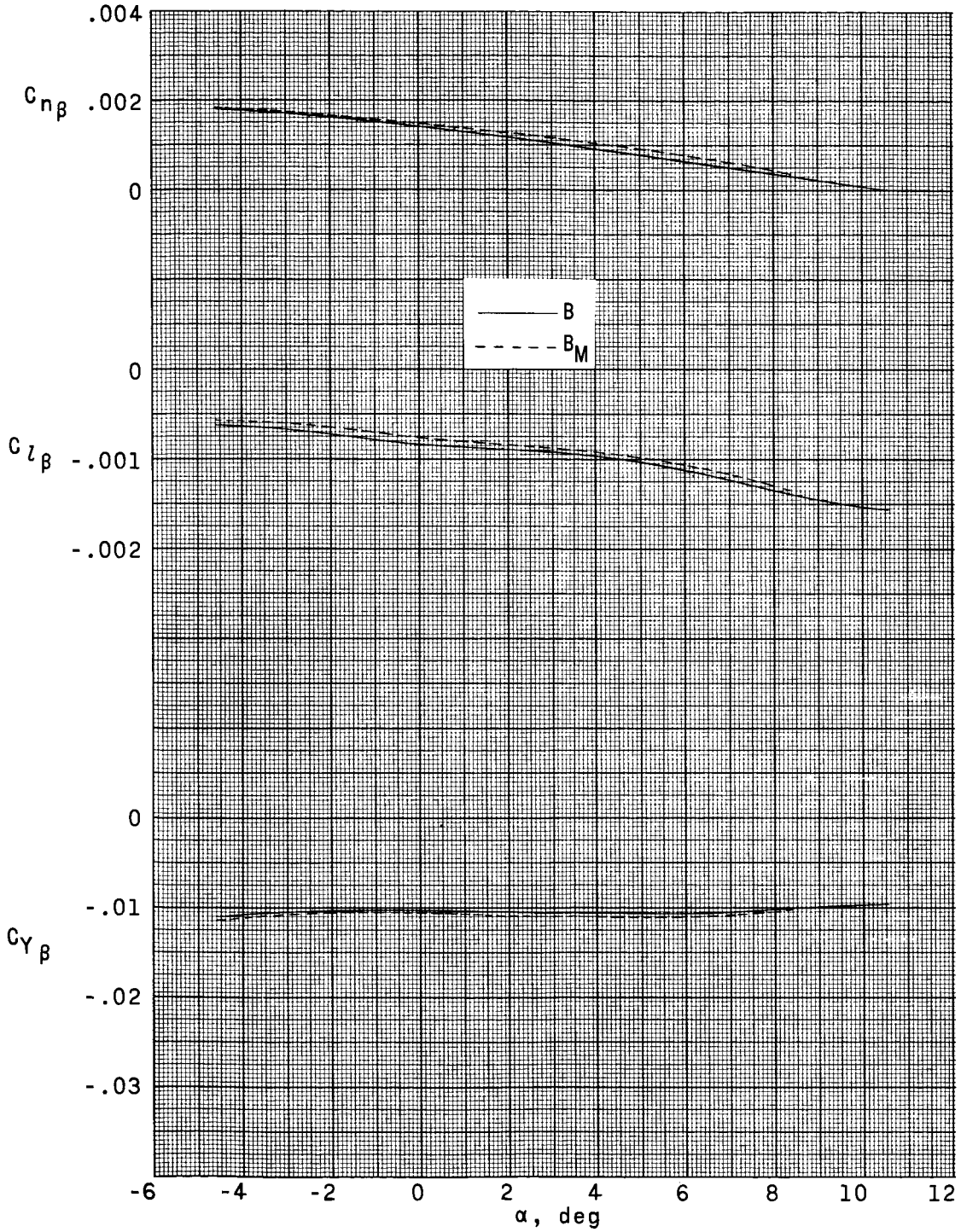

(c) M = 2.96.

Figure 10.- Concluded.

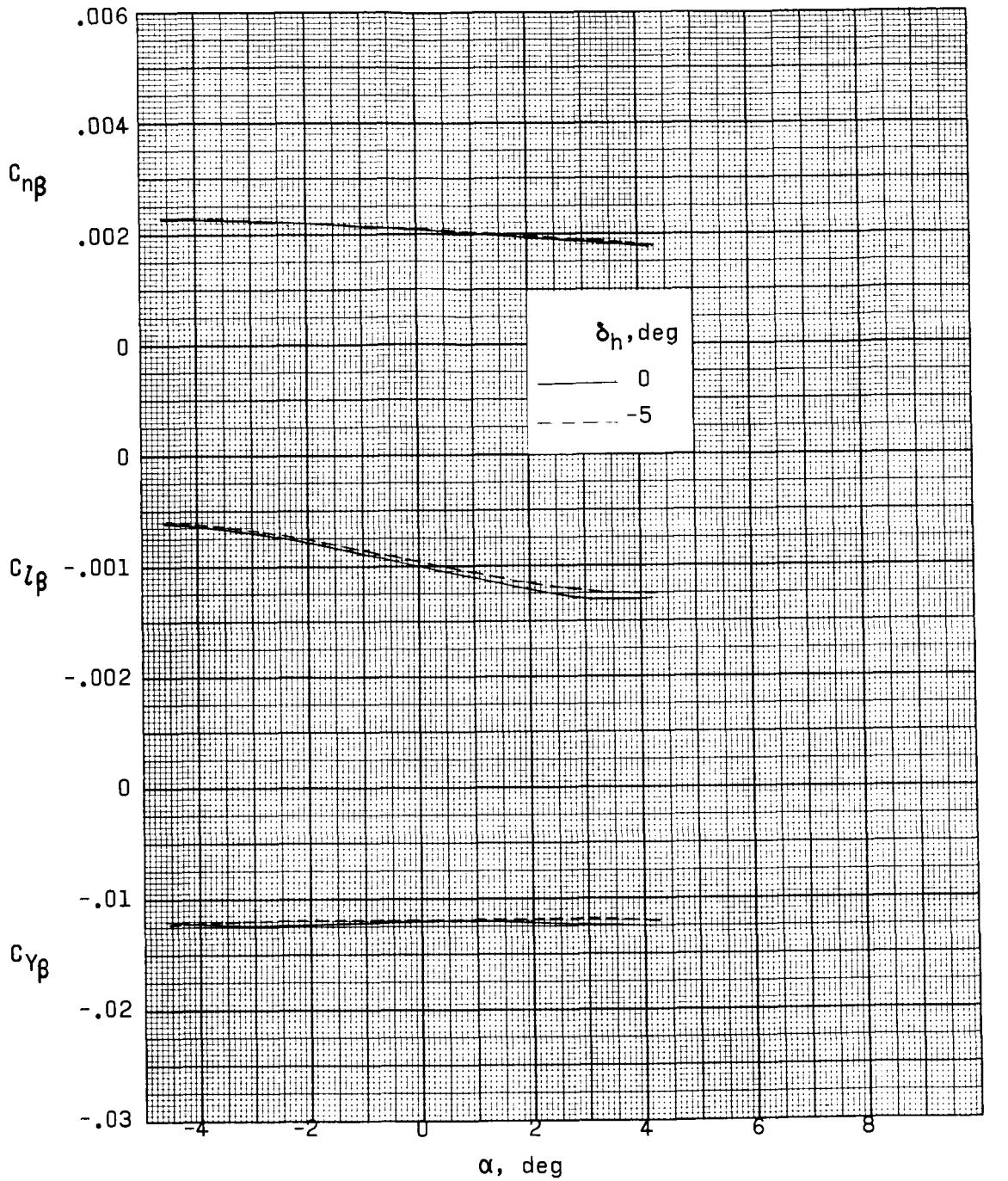

(a) M = 2.40

Figure 11.- Effect of horizontal-tail deflection on the sideslip derivatives for the configuration with modified body shape and wing glove 2. $\Lambda = 70^{\circ}$.

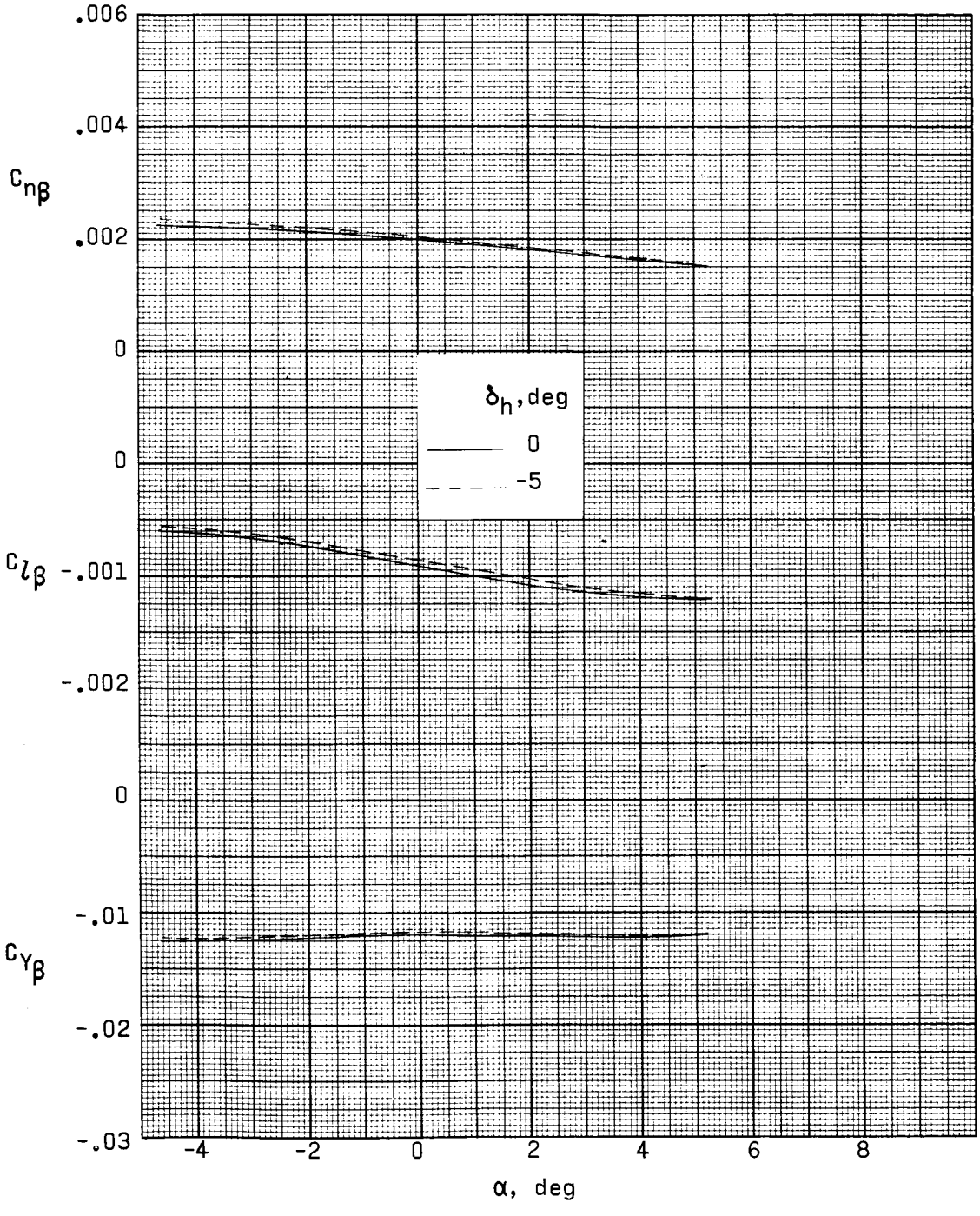

(b) M = 2.60.

Figure 11.- Continued.

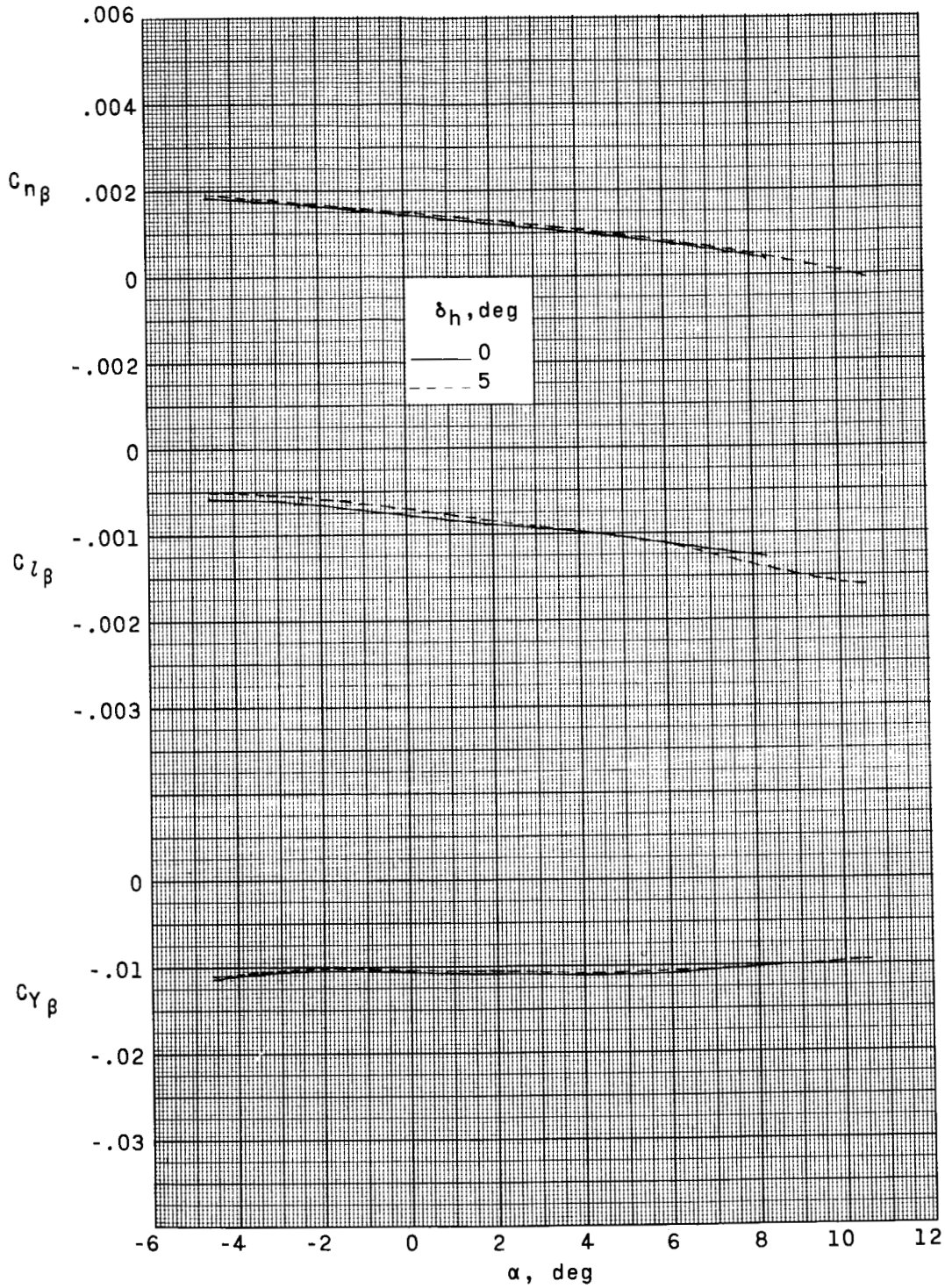

(c) M = 2.96.

Figure 11.- Concluded.

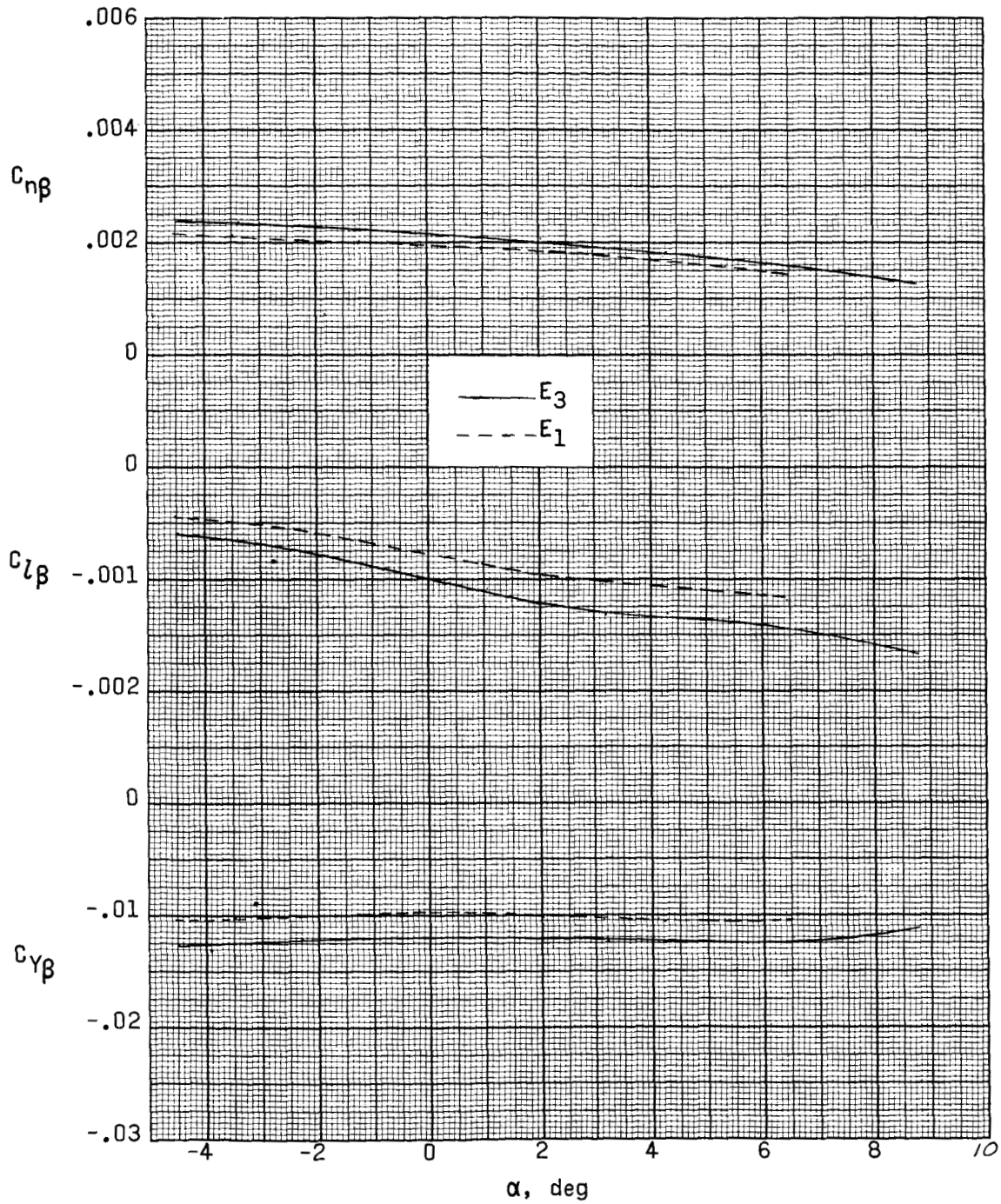

(a) M = 2.40.

Figure 12.- Effect of removing the two wing-mounted engines on the sideslip derivatives for the configuration with modified body shape and wing glove 2. $\Lambda = 70^{\circ}$.

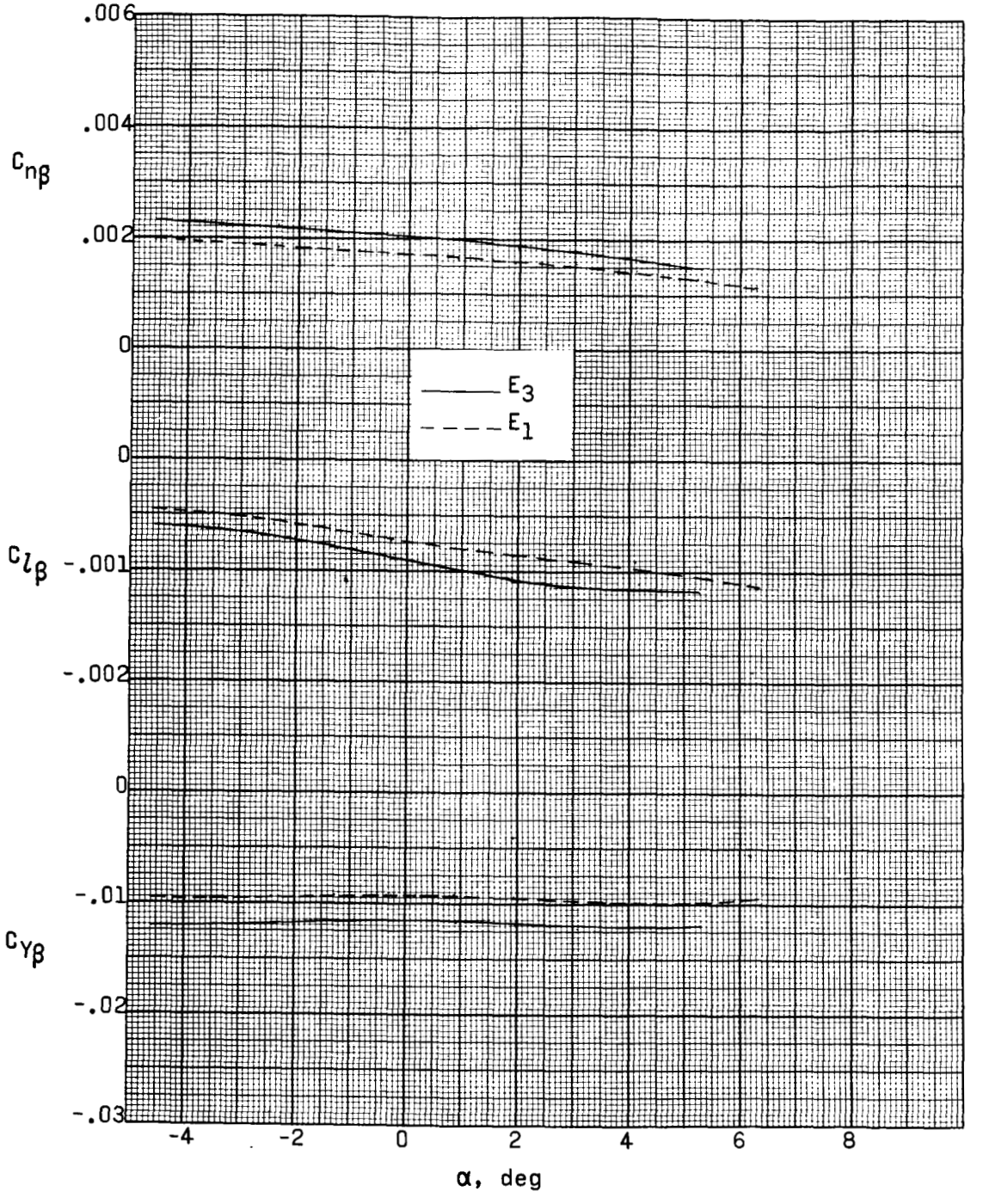

(b) M = 2.60.

Figure 12.- Continued.

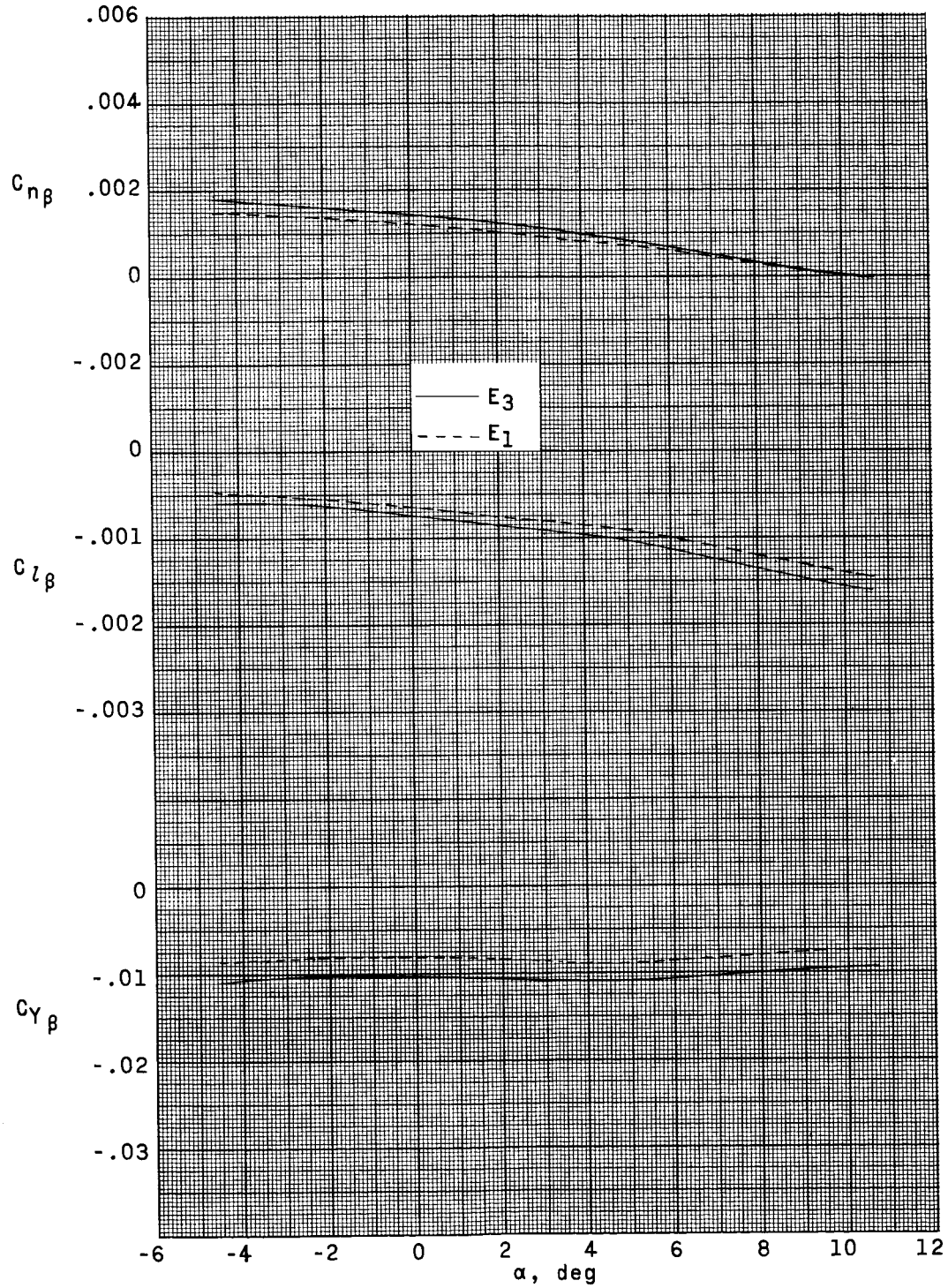

(c) M = 2.96.

Figure 12.- Concluded.